A review on the Proton-Exchange Membrane Fuel Cell break-in physical principles, activation procedures, and characterization methods

F. Van Der Linden[1,2], E. Pahon[3], S. Morando[1], D. Bouquain[2]

[1]SYMBIO, Vénissieux, France

[2]FEMTO-ST Institute, FCLAB, Univ. Bourgogne Franche-Comté, CNRS, Belfort, France

[3]FEMTO-ST Institute, FCLAB, Univ. Bourgogne Franche-Comté, UTBM, CNRS, Belfort, France

fabian.van-der-linden@symbio.one; elodie.pahon@utbm.fr ; simon.morando@symbio.one ;

david.bouquain@univ-fcomte.fr

Abstract— *The proton exchange membrane fuel cell (PEMFC) is an emission-free alternative to the internal combustion engine. Post-assembly, a PEMFC must be "activated', to elevate and stabilize its performance to a reproducible threshold value. This procedure is costly, time-consuming, and not suited for mass-production. This paper provides a detailed review of the break-in physical principles, activation procedures and characterization methods. First, all sparse knowledge from the literature is translated into a set of activation mechanisms. Activating a cell mainly alters the membrane electrode assembly morphology (e.g. catalyst layer porosity, catalyst size, shape and activity, polymer chain orientation). Second, an in-depth analysis off all break-in methods is provided. Cell components can be pre-activated using steam, acid, plasma or through compression. Dynamic, high temperature/pressure and supersaturated operation promote break-in kinetics. Generating oxidizing and reducing conditions is essential, and is achievable by short circuit, Cyclic Voltammetry, cathode starvation or reactant switch. Uniform activation over the cell surface is obtained with gas flow direction reversal or hydrogen pumping. Compression cycles minimize PEMFC contact resistances. Finally, deficiencies of conventional break-in characterization methods (to measure cell performance and impact on durability) are highlighted. Better reproducibility is achievable using advanced electrochemical characterization, post-mortem and cell output species analysis.*

Keywords—*PEMFC, Break-in, Activation, Conditioning, Procedure optimization*

Glossary

PEM	*Proton Exchange Membrane*
CL	*Catalyst Layer*
CCM	*Catalyst-Coated Membrane*
GDL	*Gas Diffusion Layer*
MPL	*Micro Porous Layer*
BP	*Bipolar Plate*
MEA	*Membrane Electrode Assembly*
PEMFC	*Proton Exchange Membrane Fuel Cell*
PolCurve	*Polarization Curve*
EIS	*Electrochemical Impedance Spectroscopy*
CyV	*Cyclic Voltammetry*
LSV	*Linear Sweep Voltammetry*
OCV	*Open Circuit Voltage*
ECSA	Electrochemically Active Surface
TPB	*Triple Phase Boundary*
CV	*Constant Voltage*
CC	*Constant Current*
ORR	*Oxygen Reduction Reaction*
HER	*Hydrogen Evolution Reaction*
COR	*Carbon Oxidation Reaction*
Pt	*Platinum*

1. Introduction

Proton exchange membrane fuel cells (PEMFCs) are among the key solutions to reducing the world's dependence on fossil fuels, especially in the heavy-duty mobility sector. Over the past decades, the cost of PEMFC systems has dropped significantly [1], owning to a variety of innovations that improved cell performance and durability [2], [3]. This leap towards technological maturity, combined with recently announced public incentives [4]–[6] have incited multiple industrial actors to invest heavily in the PEMFC. Their ambitious strategy is to further reduce the fuel cell unit cost by rapidly reaching high volume production levels [7]. However, by most estimates, these efforts will not be sufficient to achieve economical viability if the current manufacturing methods remain unchanged [1]. To truly reach a sustainable PEMFC production model, its manufacturing process must further be optimized.

At present, the most costly and time-consuming procedure on a PEMFC assembly line, and therefore a focal point for industrial actors, is the “break-in” phase. This critical step of the PEMFC manufacturing process, also called conditioning, activation, commissioning, or incubation is required for the produced cells to achieve high, stable and iso-performance. The process typically begins by placing the newly assembled fuel cell stack on an activation bench, where it is connected to an electric load, a cooling system, and supplied with reactants. Next, an activation protocol is applied, in which the fuel cell produces power by following a predetermined current or voltage profile for multiple hours [8], [9]. During this period, the performance of the fuel cell increases until reaching a plateau value. At this point, the PEMFC is broken-in and ready for operation.

To reduce the cost related to the aforementioned activation procedure, two optimization efforts have been made in the recent years, which mainly focus on the reduction of its duration and its hydrogen consumption [10]. This has driven the development of specific activation procedures, which are generally classified as “smart” or “optimized” or “accelerated” [11], [12].

Various accelerated protocols have been proposed in the literature. They consist, for example, in simply adjusting the operating conditions of the fuel cell, to profiles that induce break-in morphological changes, such as high or cyclic temperature and pressure operation. Others are moving towards the use of new equipment, to for example pump hydrogen in the cell [13]–[15] or force cathode potential cycles [16], [17]. Still others are inspired by fuel cell degradation mechanisms to activate the stack, such as carbon monoxide injection and oxidation [15], [18], forcing cathode starvations [19]–[21], or shorting the stack [22]–[24].

Despite the contributions these new methods bring towards the reduction of the fuel cell activation cost reduction, their optimization potential remains limited. Indeed, due to the general lack of knowledge on the different activation mechanisms and the impact of different stressors on the break-in kinetics, most of these protocols are based solely on trial-and-error experimental observations [9]. This implies that the interpretations of their results remain relatively uncertain and inconclusive.

Some studies on the physical principles of fuel cell activation are presented in the literature, the objective of which is to obtain a better understanding and control over the break-in mechanisms [12], [25]–[27]. Of particular interest in this regard are the papers recently published by Christmann *et al.* [11] and Pei *et al.* [28]. These publications provide a more detailed vision of the evolving interconnections between the Membrane Electrode Assembly (MEA) components, as well as the morphological changes undergoing within each layer of the cell. In general, however, most research on this topic supplied by the literature remains poorly defined, incomplete, or outdated.

Furthermore, as the interest in the PEMFC activation phase remains recent, other matters are not sufficiently addressed in the literature. This includes the lack of break-in diagnosis tools [21], normalized end-of break-in criteria (e.g. performance threshold, convergence, decay..) and post-activation characterization methods [29]. Other aspects such as the impact of activation protocols on stack durability [30] or the effects of stack specifications on its activation kinetics [31], [32] also deserve more attention.

To the best of our knowledge, no paper that covers, profoundly studies, and combines all aspects of PEMFC activation (e.g. break-in mechanisms, procedures, characterization, ageing...) exists in the literature. Yet, such an article is essential as a solid foundation for future research on break-in protocols and for developing optimized solutions. Providing the literature with that fundamental basis is the objective of this review paper.

Including this brief introduction, the study is organized into five sections. In the second section, all the currently known fuel cell break-in mechanisms are defined and dissociated. This amounts to combining all the scattered knowledge and experimental results supplied by the literature and establishing several additional theoretical explanations. In the third section, all the break-in methodologies and their associated characteristics (e.g. used machinery, operating conditions...) are presented. This section is accompanied by a detailed analysis of each activation method, by linking each stressor to the break-in mechanisms that are listed in the previous section.

The fourth section is devoted to the characterization of PEMFC break-in. Its first lists all the apparatus and methodologies that can be used to monitor the progress of individual activation mechanisms, in order to determine the "state of activation". This is followed by a detailed review of methods for comparative evaluation of break-in protocols, with an emphasis on the influence of stack characteristics on benchmarking results. The fifth and final section concludes this review, and provides perspectives to further optimize fuel cell break-in.

2. PEMFC break-in physical principles

In the literature, the mechanisms behind fuel cell break-in are often defined as the hydration of the membrane and the "activation" of the catalyst layers (CLs). This vague definition illustrates the lack of knowledge that currently exists in this area. Nor does it explain why it takes multiple hours for a fuel cell to reach high and stable performance (to be "broken-in"). Nevertheless, put together, the sparse research provides good theories to explain break-in mechanisms [11], [26], [27]. In this section, the different morphological changes undergone by a fuel cell during activation are presented one by one.

2.1. Membrane activation mechanisms

To explain the polymer electrolyte break-in process, a quick introduction is given to its composition and its working principle. In the membrane, water is transported through hydrophilic chains containing SO_3^- sites, also called "active sites", which can be in a protonated state. More active sites (more SO_3^- sites within the ionomer) results in a higher water content and thus a better proton conductivity. A hydrophobic backbone is required to "hold" the SO_3^- containing side chain and to ensure mechanical and chemical stability. To further increase mechanical stability, a chemical inert layer or "reinforcement" additives can be used to prevent multi-dimensional swelling. To further increase chemical stability, "radical scavengers" are added to neutralize radicals before they interact with the side chains. A detailed presentation of the ionomer molecular structure is given in [11].

The membrane water content (noted λ), corresponds to the number of water molecules per SO_3^- site [33]. It can be dissociated into three different regions, which are residual, bound and free water, where:

$$\lambda_{tot} = \lambda_0 + \lambda_B + \lambda_F \quad (1)$$

Residual water (λ_0) forms the primary solvent shell. It possesses a strong bond, changes only at higher temperatures, and is often neglected as it does not vary with cell humidity conditions.

Bound water (λ_B) regimes form around the primary shell, with a water content up to 6 water molecules per SO_3^- site. Free water (λ_F) regimes form with the increase in water domains and higher connectivity between the domains.

The gain in fuel cell performance related to membrane activation is typically explained by its increase in water content (λ), and consequently its proton resistance reduction. The membrane break-in process is actually much more complex, as it also involves swelling, polymer relaxation, decontamination, domain spacing, surface skin change, etc. [34]. These activation mechanisms are presented in the following subsections.

2.1.1 Membrane activation mechanisms: Polymer hydration and structure change

The different "extreme" environmental conditions (humidity, pressure and temperature related) that the membrane goes through during its production enforces a thermal and swelling memory. This memory imposes a certain membrane crystallinity level, which in turn defines its maximum water uptake capacity in the free water regime region (λ_F). After production, the high crystallization degree results in low ionomer domain spacing, hindering water uptake, swelling and the mobility of the side chains and backbones [11].

When it is firstly hydrated during break-in, the ionomer structure undergoes multiple changes. The water domains in the membrane progressively grow and deform the polymer matrix, generating a swelling pressure.

Figure 1(a) is a schematic representation of the microstructure evolution undergone by the membrane water clusters during activation [35]. When two clusters coagulate: (i) the channels connecting the two clusters is diminished and (ii) the content of free water (λ_F) in the cluster increases (iii) distances between the sulfonate groups are reduced. These all contribute to minimize the energy barrier for proton transport.

Forming the continuous water network throughout the membrane is a sluggish process. It mainly depends on the time required for domain spacing (over 200 min) and polymer matrix relaxation (two to three orders of magnitude higher than the diffusion time constant). Kusoglu *et al*. have expressed the different processes

(diffusion, polymer relaxation, domain spacing...) using an empirical fickian equation, where a different time constants is attributed to each process [34]. On

FIGURE 1(b), inter-domain spacing and consequently the size of the water domains increase with time is shown.

2.1.2 Membrane activation mechanisms: Polymer surface skin rearrangement

The state of the membrane surface skin has a decisive impact on the diffusion rate within the polymer, and must be rearranged during activation. When firstly producing and/or injecting water in a fuel cell, liquid water is formed at the ionomer surface. This transforms the membrane surface skin, by aligning the polymer bundles perpendicular towards the surface. The ionic conductive sites form a more hydrophilic skin layer, enhancing proton transport, reducing surface tension and therefore accelerating water uptake. The dependency of sorption kinetics on the water phase at the membrane surface, is known as the Schroeder paradox[1].

Apart from rearranging the polymer bundles, the formed liquid water film also ensures the connection between the membrane skin layer and the environment, therefore reducing proton transport resistance [11].

2.1.3 Membrane activation mechanisms: Polymer decontamination

After its production, the fuel cell membrane is contaminated with a certain number of impurities, additives, and other particles. These species reduce proton conductivity, affect electro-osmotic drag (water transported by the H^+ flow [36]) and can moderately to severely affect cell performance. There is for example an excess of chemical additives (metal oxides and chemical complexes) which must be evacuated. Indeed, as previously stated, the membrane is doped with additives to mitigate chemical degradation, but they are often added to an excess to guarantee membrane chemical stability [37], [38]. Depending on the pre-break-in cell and/or membrane storage conditions, airborne species may also have contaminated the membrane [12]. The same goes for dust particles or other residues from the production step. Further in-situ contamination during the first start-up process

[1] Schroeder's paradox: Nafion water uptake is different when exposed to vapor and liquid at the same activity

must also be mitigated [11]. Indeed, as the cell voltage levels typically vary during break-in, this can generate metallic cations, which in turn can be introduced within the membrane.

During activation, the generated water and proton flow both contribute to the mechanical migration and extraction of impurities [39]. Conveniently, in-situ metallic cations contamination during activation is also mitigated by a high water production and high relative humidity (RH) [11]. The removal of all contaminants from the membrane can however be a slow process (multiple hours).

As stated above, membrane decontamination increases proton conductivity to a certain extend. The most significant impact of membrane decontamination on cell performance is however related to the proton resistance and ORR (oxygen reduction reaction) kinetics at the cathode CL. This will be discussed in further detail in the following section, dedicated to the CL activation mechanisms.

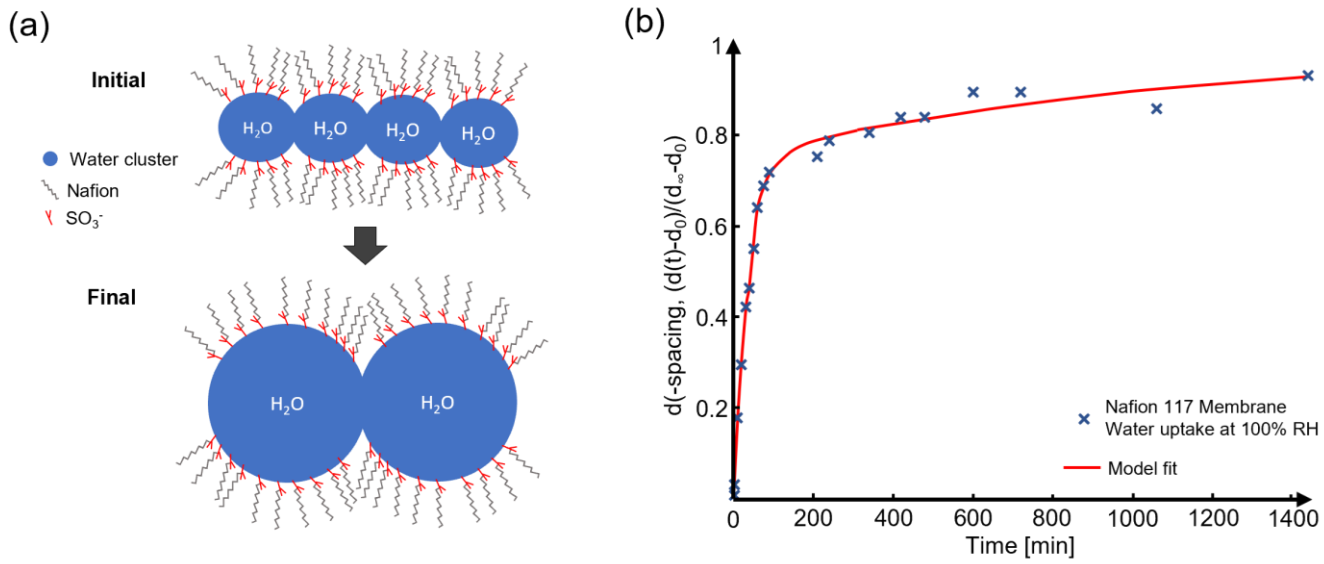

FIGURE 1. MEMBRANE ACTIVATION MECHANISMS: (A) COAGULATION OF TWO WATER CLUSTERS DURING BREAK-IN WITH INCREASING CURRENT DENSITY [35], (B) SWELLING OF WATER DOMAINS WITH TIME FOR A MEMBRANE EXPOSED TO SATURATED WATER VAPOR AT AMBIENT TEMPERATURE [34]

2.2 Catalyst layer activation mechanisms

As previously stated, the CL is a multicomponent porous structure containing polymer, carbon black and Platinum (Pt). The regions where all elements connect are called active sites (not to be confused with the SO_3^-

sites of the polymer) or three phase points. Nafion is typically used in the CL, to transport the hydrogen ions to and from the active sites.

The CL structure strongly affects overall cell performance, and is subjected to multiple structural changes during break-in. They concern all individual CL components (ionomer, carbon, catalyst and pores for gas diffusion) and are presented throughout the following subsections.

2.2.1 Catalyst layer activation mechanisms: Pore structure change

The most common CL production method consists of directly dissolving Nafion with iso-propyl alcohol (IPA), to then be mixed with the carbon supported catalyst. This is to achieve a homogeneous distribution of the ionomer. This production method does not guarantee access to reactants, electrons, and protons in every region of the CL. Furthermore, particles, excess ionomer, and other impurities that are not anchored may also hinder the reactant diffusion and must be evacuated [11]. Nowadays, to increase the catalyst surface in the CL, the Pt nanoparticles are not only deposited on the outer surface of the carbon support, but also within the carbon cores via internal pores [40]. Unanchored particles may hinder the accessibility of the Pt located within these micropores.

During break-in, the reactants, heat and water transport evacuates the unanchored particles from the CL, but also directly affects the CL structure. The total number and volume of pores increase (porosity) as well as the number of twists and bends in those pore channels (tortuosity). Pore shape may also be affected [27]. This enhances the reactants mobility and therefore, reduces mass transfer resistance. This may be not limited to the CL, as it may also include the Gas Diffusion Layer (GDL) and Micro Porous Layer (MPL). The pore opening, accompanied by the evacuation of unanchored particles also increases the number of active sites by opening new pores leading to formerly “dead regions” [26]. This enhances the cell mass activity (mA.mgPt-1), and more specifically the total electrochemically active surface (ECSA) (m^2.gPt-1).

2.2.2 Catalyst layer activation mechanisms: Polymer hydration and structure change

Like the membrane, the polymer in the CL must be hydrated during break-in to enhance its proton conductivity. Increasing the CL polymer water content during activation is also essential for three other reasons, which are ionomer swelling, side chain reorientation and gas permeability increase.

The swelling pressure generated by the growth of water domains in the CL ionomer during break-in deforms and expands the polymer matrix. Maximizing the ionomer footprint increases the number of active sites as the electrolyte introduces into the CL. Ionomer swelling also increases the triple phase boundary (TPB) per active site, as it surrounds a larger surface of the Pt particle [10]. The joining between the different ionomer sections may also reduce the proton transport resistance between the CL and the membrane.

During break-in, as soon as water is produced, the polymer side chains orient themselves towards the Pt surface. This reorientation occurs due to the catalyst hydrophilic character, and improves the proton conductivity inside the CL [11]. Simultaneously, the production of a thin water film between the ionomer and the catalyst supports proton conductivity near the active sites, as well as the ORR activity.

Even though ionomer is an essential component in the CL, it negatively affects the mass transfer resistance. Indeed, it hinders the reactant accessibility to the active sites, as they must diffuse through the thin ionomer layer to reach the catalyst [41]. Oxygen diffusion resistance through the ionomer and to the Pt surface may even be the dominant loss compared to oxygen transport resistance through the GDL and CL pores [42]. The amount of ionomer in a CL is therefore limited, to obtain an acceptable compromise between proton conductivity and oxygen permeability.

FIGURE 2(a) and

FIGURE 2(b) illustrate the local oxygen transport resistance of the polymer on the Pt, and the decomposition of the associated PEMFC mass transport voltage losses, respectively.

When the CL polymer hydrates during activation, its oxygen transport resistance reduces. Indeed, the ionomer phase-separates in aqueous and hydrophobic (polymer-backbone) rich domains. The gas permeability of the aqueous phase is an order of magnitude greater than that of the hydrophobic domain. The thin water film produced on the catalyst surface may also enhance the oxygen transport properties. Indeed, it mitigates direct sulfonate-Pt interaction, which is detrimental to oxygen transport near the Pt surface [41].

This said, some opposing views exist regarding the polymer hydration effects and fuel cell performance increase. This is especially true for the oxygen transport resistance at the interface of the ionomer in contact with the catalyst. For example, a too thick water film between the catalyst and the ionomer may deteriorate the oxygen transport rate [11]. The water film may also hinder water uptake in the second layers (good proton conductivity is required over the whole catalyst structure and not only the catalyst sites). Polymer side chain reorientation at the Pt interface may also favour the sorption of end groups on the catalyst surface and so further hinder oxygen diffusion. The CL polymer hydration mechanisms are still open for debate and must therefore be further studied.

2.2.3 Catalyst layer activation mechanisms: Carbon support oxidation

On the CL carbon support, defect sites (C^+) which are prone to electrochemical oxidation may form C-OH groups. Consequently, carbon surface oxides may take shape on the catalyst surface (CO_{surf}) and then be oxidized to CO_2. This conversion process is defined as the carbon oxidation reaction (COR), and results in the loss of carbon support (**Erreur ! Source du renvoi introuvable.**). The COR typically occurs in a high potential environment (above 0.6V), which is achievable in a PEMFC.

During activation, if the fuel cell is supplied with fuel (H_2/air) and no/little current is drawn from it, the high cathode potential initiates the carbon support oxidation reaction (COR). According to Kim *et al*. [10], the COR is partly responsible for the TPB increase in the CL during break-in. The loss of carbon support increases the bond between the catalyst and the ionomer surrounding the Pt particles. If the carbon supporting the Pt particle disappears, catalyst rearrangement may even occur, as it relocates to the ionomer. This increases the contact surface at the catalyst-ionomer-gas conversion point [19].

TABLE 1. CO_2 FORMATION THROUGH THE CARBON OXIDATION REACTION (COR) [10]

Expression
$C \rightarrow C^{+}_{(s)} + e^{-}$
$C^{+}_{(s)} + H_2O \rightarrow CO_{surf} + 2H^{+} + e^{-}$
$CO_{surf} + H_2O \rightarrow CO_2 + 2H^{+} + 2e^{-}$

When the carbon black is oxidized, its hydrophilic/hydrophobic properties are also affected. According to Kocha *et al*., improving the carbon support hydrophilic properties is required to obtain reproductible performance [12]. The increase of carbon hydrophobicity may also accelerate the CL ionomer hydration and surface skin rearrangement.

The enlargement of the TPB area by the COR is debatable. Indeed, the COR is typically considered as a severe fuel cell degradation mechanism for the following reasons: (i) Pt particle relocation results in the loss of the electron conductor phase, hindering electron transport. (ii) The loss of carbon support can also result in loss and/or agglomeration of catalyst particles and consequently a reduction of ECSA. (iii) The intermediate products of oxidation (CO_{surf}) may remain on the surface of metal catalyst particles and poison the catalytic sites with a subsequent loss of ORR activity [43]. (4) Reducing the hydrophobic properties of the carbon surface increases water transfer resistance resulting in less efficient reactant transport [12]. The necessity of carbon support oxidation to obtain reproductible performance, as well as its beneficial and detrimental effects during break-in must be further studied.

2.2.4 Catalyst layer activation mechanisms: Catalyst decontamination

When a fuel cell is just assembled, many unwanted species are found on the catalyst surface. This “poison layer” or “impurity layer” adversely affects the ORR [41] and limits the active surface [44]. These species, their nature and their origins are presented below.

As previously stated, a certain number of chemical complexes are flushed out of the membrane during fuel cell activation. As they are drawn toward the cathode CL, these impurities progressively adsorb on the Pt, which affects the ORR [41], [45]. The amplitude of the catalyst contamination by the ionomer chemical additives depends

on their nature (more severe with organic than inorganic additives) [37], [38]. With inorganic additives however (e.g. M-MnO_2), produced ions (e.g. Mn^-, Mn^{2+}) irreversibly interact with the sulfonic acid sites, resulting in lower final polymer proton conductivity [46]. Apart from chemical additives, other membrane compounds such as sulfonate groups and fluoride are drawn to the CL during break-in. A fraction of these species may be trapped in the MEA after production, and others may be formed during the break-in process as the membrane slightly degrades [41]. Carbonaceous species derived from alcohol, if the latter has been used to form the catalytic ink also contaminate the catalyst. A solution based on iso-propyl alcohol is typically used, for its quick and effective evaporation. When alcohol evaporates, it transforms into hydrocarbons and thus poisons the CL [47]. If solvents do not properly evaporate, the oxygen diffusion may also negatively be affected.

In addition to the contaminants derived from the MEA components, airborne species also contaminate the catalyst surface, and must be desorbed during break-in. A fuel cell manufacturing process typically includes extended storage periods of stacks or cell components, during which the catalyst is slowly being poisoned by the surrounding air [44]. Sulfur oxides (SO_x), nitrogen oxides (NO_x), carbon oxides (CO_x), propane, benzene and many other organic chemical species partly settle in the catalyst [45]. Poisoning occurs at extremely low concentration of impurity anions such as sulfate, chloride and nitrate (starting at 500 ppb for sulphur dioxide for example) [48]. Among air contaminants, S impurities (H_2S and SO_2) have been shown to cause the most important performance decay. Apart from airborne contaminants, a thick layer of surface oxides on the Pt surface also hiders the ORR. The amount of coverage and type of oxide species is mixed (PtOH, PtO, PtO_2 etc…). In addition to the surface oxides, there is a slow logarithmic growth of sub-surface oxide layers, via the “place exchange mechanism” [41], [45].

Catalyst decontamination corresponds to the desorption and removal of all previously mentioned surface-blocking species. This break-in mechanism is essential as it strongly increases the catalyst ORR and mass activity [41] and in turn severely affects cell performance. The oxide removal process is relatively quick and can take from a few seconds to 20 minutes [49]. As demonstrated through Electrochemical Impedance Spectroscopy (EIS) measurements during the performance recovery phase of a doped MEA, the desorption rate of chemical additives is more sluggish [38].

2.2.5 Catalyst layer activation mechanisms: Catalyst structure reorganization

To maximize the Pt surface to mass ratio ($m^2.gPt^{-1}$) and consequently the ECSA, Pt particles are machined into small spheres. The adsorption of oxygenated species in the catalyst surface however increases inversely proportional to Pt particle size. Thus, an optimal Pt particle size exists (2 to 4nm), where the ECSA is maximized, and the ORR is not hindered by the strong adsorption of oxygenated intermediate species [11].

Pt particle deposition on the carbon surface is not perfectly homogeneous. Consequently, Pt particles reorganize during activation, to reduce surface energy irregularities. During reorganization, Pt particles irreversibly increase in size through migration, agglomeration, and coalescence as well as Pt dissolution from the support and redeposition. The amplitude of each contribution depends on the size and location of the Pt on the carbon support, carbon support type, and the nature of the Pt-C interface [41].

Even though during break-in, the increase in Pt particle size reduces the ECSA ($m^2.gPt^{-1}$), an overall increase in mass activity ($mA.mgPt^{-1}$) is observed. This can partly be explained by the counterbalancing effect of other activation mechanisms such as catalyst decontamination, which increase the "specific activity" or activity per site ($A.cmPt^{-2}$). This said, the catalyst structure reorganization is also partly responsible for the increase in mass activity. Figure 2(c) illustrates the counterbalancing effect Pt contaminant removal has on the Pt particle growth, in terms of Mass activity evolution.

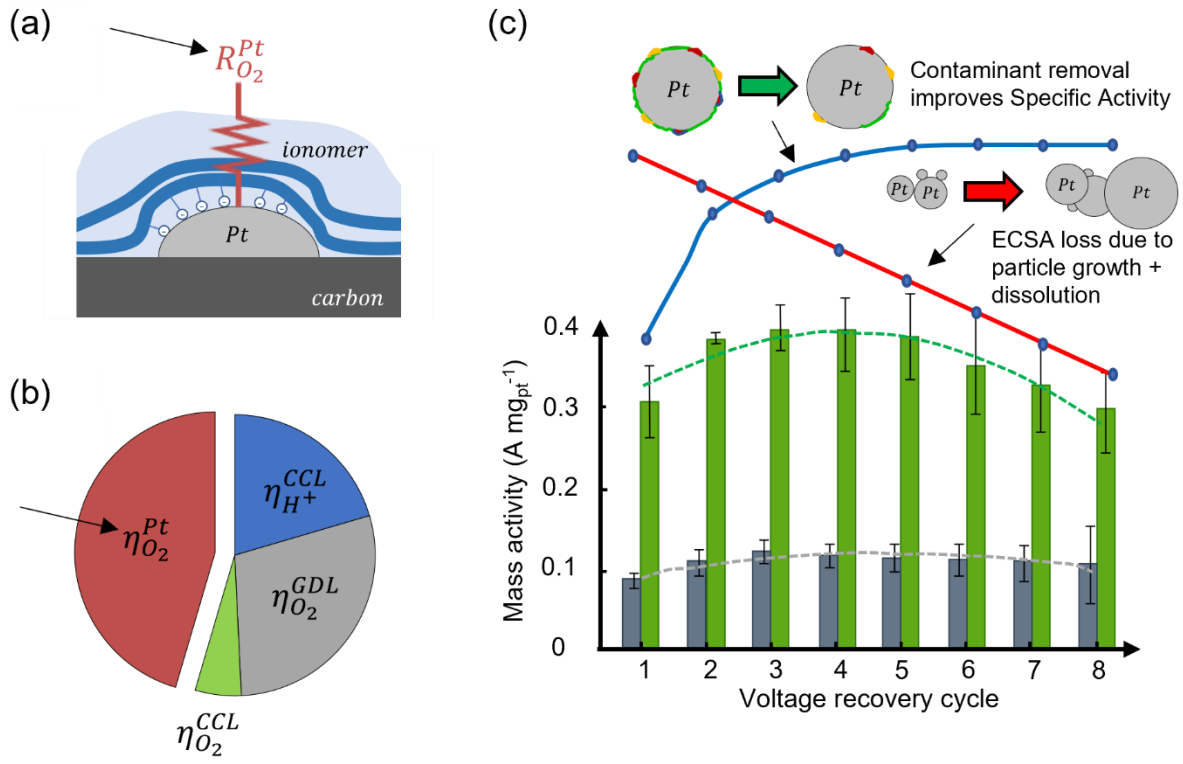

FIGURE 2. CL ACTIVATION MECHANISMS: (A) LOCAL O_2 TRANSPORT RESISTANCE (R_{O_2}) ON PT, (B) DECOMPOSITION OF PEMFC MASS TRANSPORT VOLTAGE LOSSES (η) [42], (C) COMBINED EFFECTS OF CATALYST DECONTAMINATION AND ECSA LOSS ON FUEL CELL MASS ACTIVITY DUE TO PARTICLE GROWTH [41]

First, Pt dissolution may counter intuitively locally increase the ECSA, by dissolving Pt particles which block pores leading to formerly "dead regions" [11]. Second, by affecting the Pt structure sensitivity of the ORR, catalyst reorganization results in an increase in activity per site ($A.cmPt^{-2}$) [41]. Indeed, the increase of Pt particle size reduces the adsorption strength of oxygenated species (O, OH, OOH…), in favour of the ORR [11]. Furthermore, the rearrangement of catalyst particles also results in the rearrangement of the catalyst atomic structure (Pt-Pt and Pt-Cobalt coordination) [41], decreasing the Pt-O bond strength [49].

Third, as previously stated, before activation, a layer of subsurface Pt-oxides exists, which has been formed due to the place-exchange mechanism. At the start of break-in (first 20 minutes), as the Pt oxide dissolution is enhanced, sub-surface Pt is exposed, leading to a greater Pt surface roughness. During the following 200 minutes, the corners of the Pt particles are progressively rounded, and the rough faces are smoothed, therefore increasing the ORR mass activity [49].

2.3 Cell activation mechanisms

The individual PEMFC components are the Catalyst-Coated Membranes or CCMs (composed of the Proton Exchange Membrane or PEM and its CLs), porous layers (GDLs with MPLs), Bipolar plates (BPs) and sealing gaskets [50]. To assemble the cell, all components are sandwiched and then clamped together at a certain predetermined pressure value. This seals and isolates the cell and maintains an adequate contact surface area between all components.

The cell ohmic resistance corresponds to the cumulated resistances of each component (of which the membrane has the highest value), but also the contact interface resistances between cell components [27]. During activation, the contact surface area between all components, and therefore the cell contact interface resistances evolve. This section may be referred to as the "mechanical" aspect of fuel cell break-in.

2.3.1 Cell activation mechanisms: Interfacial contact resistance reduction

The interfacial contact resistances between cell components are significant contributors to the ohmic losses in PEMFCs. According to Netwall *et al*., they may even be the main contributor to the total cell ohmic losses [50]. The contact resistance between the GDL and BP is considered as the most significant, and therefore causes the highest potential loss [51]. This said, the surface contact resistances between the microporous, catalyst, and ionomer layers are also not negligible. Their values however rather depend on the MEA production methods and conditions (temperature, pressure, duration..), than stack compression [52], [53].

Before activation, the freshly assembled cell components have not had a chance to adapt and fit to each other's forms. Furthermore, as previously stated, during break-in, irreversible morphological and microstructural deformations/changes and variable water and heat production take place. Both points alter the cell contact interface resistances. During activation, by adjusting the stack clamping pressure, the cell components can progressively be deformed until no more variations are observed, and the minimal area-specific resistance is reached [50].

2.4 PEMFC activation mechanisms: Summary diagram and table

To conclude, multiple morphological changes occur during break-in and are mostly of an electrochemical nature and taking place in the MEA. The diagram shown in Figure 3 is a simplified representation of the morphological changes endured by the MEA during activation.

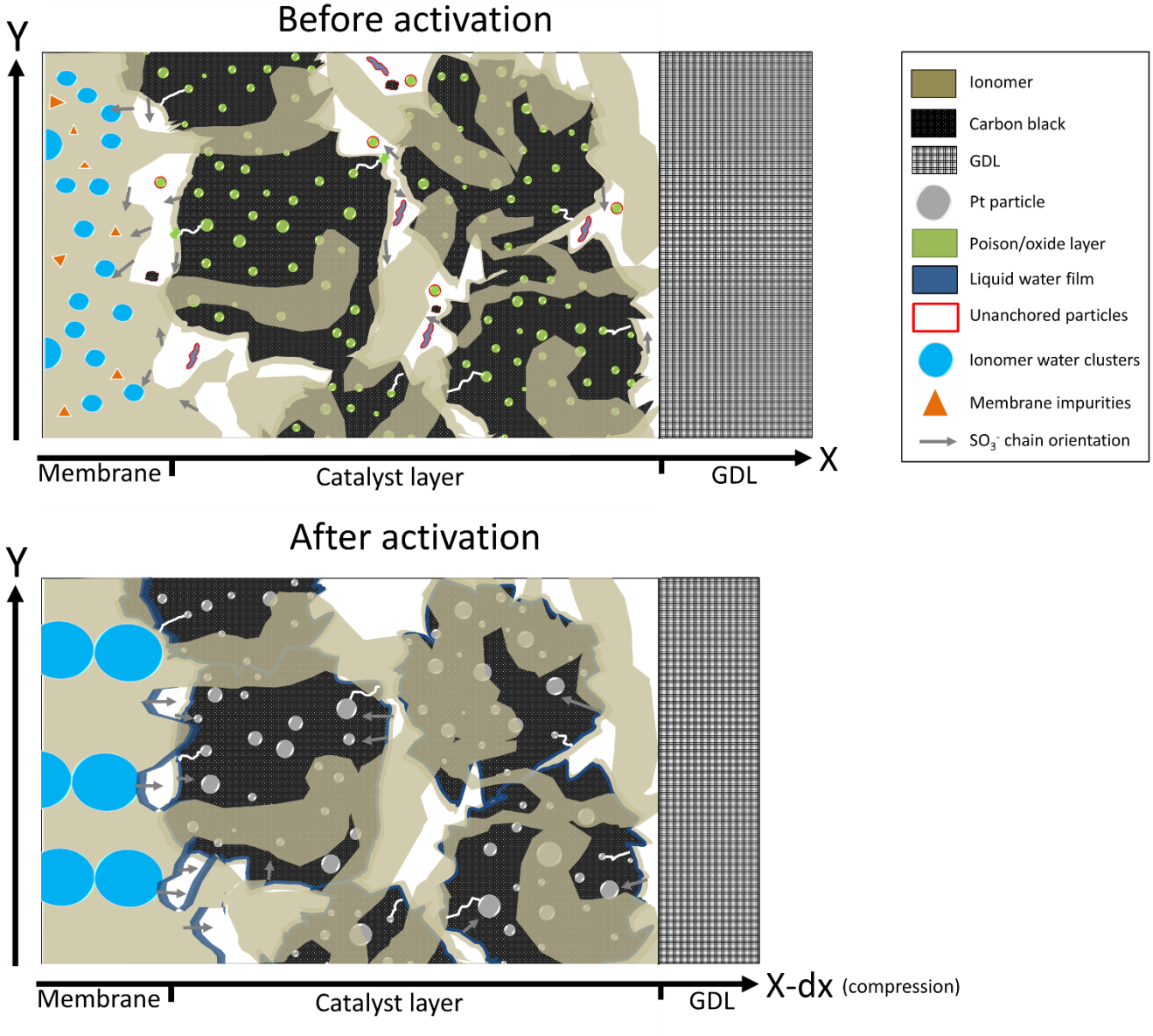

FIGURE 3. MORPHOLOGICAL CHANGES ENDURED BY THE MEA DURING BREAK-IN.

For the membrane, there is the polymer hydration and structure change, surface skin rearrangement and decontamination. For the CL, there is the pore structure change, polymer hydration and carbon support oxidation, as well as catalyst decontamination and catalyst structure reorganization. These morphological changes directly

affect cell properties such as the cell porosity, catalyst size, shape and activity, polymer chain orientation and spacing, etc. Cumulated, the break-in mechanisms contribute to reduce the entire spectrum of fuel cell resistances (reaction rate, ohmic and mass transfer).

TABLE 2. BREAK-IN MECHANISMS, ASSOCIATED TIME SCALES AND MAIN EFFECTS

Mechanism	Time scale	Main Effect
Membrane		
Polymer hydration and structure change	> 200 min	Ohmic resistance reduction
Polymer surface skin rearrangement	Max 20 min	Ohmic resistance reduction
Polymer decontamination	Hours	Ohmic resistance reduction
Catalyst layer		
Pore structure change	Minutes – hours	Mass transport and reaction rate resistance reduction (ECSA increase)
Polymer hydration and structure change	/	Ohmic and mass transport resistance reduction
Carbon support oxidation	Minutes - hours	Reaction rate resistance reduction (ECSA increase)
Catalyst decontamination	Seconds - hours	Reaction rate resistance reduction (Specific activity increase)
Catalyst structure reorganization	Hours - days	Reaction rate resistance reduction (ECSA reduction, specific activity increase)
Cell		
Interfacial contact resistance reduction	Minutes	Ohmic resistance reduction

Using the knowledge behind break-in physics (Table 2), the fuel cell activation process and associated methods can be revisited. It is essential to understand these physical principles to investigate and correctly interpret the different existing break-in methods, presented in the following section.

3. PEMFC break-in experimental methods

As stated in the introduction of this paper, the break-in process typically consists of placing the fuel cell stack on an activation bench, where it produces power by following a predetermined current or voltage profile for multiple hours. The long duration break-in step is currently the limiting factor to the fuel cell production line capacity. In response to the new gathered knowledge regarding break-in mechanisms, a certain number of “smart” or “optimized” methods have been presented in the literature. These methods typically reduce the time required

to break-in a fuel cell, or bring other improvements such as minimizing reactant consumption, simplifying the break-in process, reducing machinery cost, etc.

New activation methods are typically related with stress, by modifying the operating parameters or load profile. Some of these new methods are applied on a traditional activation bench whilst other are more exotic and use non-conventional machinery or processes. There are even methods which consist of partly integrating fuel cell break-in into the manufacturing process. In the literature, these new break-in procedures are often distinguished in two categories, which are “Online” and “Offline” activation. The definition between offline break-in (also called pre-treatment) and online break-in is however ambiguous. Some categorize pre-treatment as all protocols applied on fuel cell components before their full assembly. Others state offline methods as all protocols not requiring an electronic load and/or activation bench. In this paper, “offline” break-in, or “pre-treatment”, or “ex-situ” methods are categorized as all methods applied pre-final fuel cell assembly. The second category of “online” or “in-situ” break-in is composed of all other methods, and are applied on fully assembled fuel cell stacks (whether they require a load and/or activation bench, or not).

Efforts have been made to summarize and categorize all methods throughout the following subsections. Methods that have similarities regarding their process / operating conditions are placed in the same category.

3.1 Break-in methods applied before final Fuel cell assembly (Offline break-in)

Even though it is not carried out on an activation bench, fuel cell pre-treatment can also be classified as a partial break-in procedure, as it affects the MEA morphology. If a fuel cell is pre-treated, it still needs to be broken-in on an activation bench, but for a shorter period. Fuel cells can be pre-treated instead of waiting for the activation bench to become available, consequently increasing the production line capacity. The fuel cell pre-treatment procedures found in the literature are presented in this subsection.

3.1.1 Offline break-in: Electrode / MEA steaming / boiling

Electrode steaming/boiling involves treating the catalyst coated electrode in liquid water or steam, before MEA assembly. Using a simple household pressure cooker and 10 minutes of steaming, Kaufman *et al*. manage to

increase an initial cell performance by over 50% (at 0.6V) [54]. The steam enhances CL porosity, washes out unanchored impurities and removes excess ionomer, which eases reactant transport and opens new active sites. It may also improve the CL ionomer crystallinity level and polymer arrangement, which in turn increases the free water content and total maximum water uptake [11]. The following MEA assembly process (called hot bonding) however fully dehydrates the polymer, and sets a thermal history [55], partly erasing the effects of the pre-treatment method. Some effects of electrode steaming on the polymer structure however remain, as the CL maintains an easier hydration characteristic after MEA assembly [54].

A method that consists of steaming an entire CCM and/or MEA has also been presented in the literature [56]. This more recent patent, (owned by the 3M corporation) suggests that the steam treatment should be applied at a super-atmospheric pressure for better performance. As this method is applied after the MEA hot bonding process, it is not followed by ionomer dehydration or crystallinity increase. Other issues related to CCM swelling and deformation however arise, which might make stacking impossible or cause reactant leaks. In [57], Zhiani *et al*. state that the method can be applied on a 7-layer MEA (composed with the sub-gasket). The sub-gasket material resistance to such levels of humidity and heat also remains questionable. It therefore might be preferable to steam treat the MEA when it is fully assembled in a stack. This process will be presented later on, in the "online" break-in section.

3.1.2 Offline break-in: H_2SO_4 electrochemical treatment

This method consists of immersing a MEA in a diluted sulfuric acid solution, connecting it to a small load, and then carrying out potentiostatic and galvanostatic cycles. The potential is maintained between the limits of Pt oxide (PtO) formation (>0.8V) and hydrogen evolution (<0V). The entire operation is carried out one time to treat the anode and one time for the cathode, by switching the polarities of the two sides of the MEA. According to Palanichamy *et al*., this process may not only increase the CL porosity, but also desorbs surface-blocking species from the Pt surface [47]. Other studies suggest that when a polymer is treated with strong acids (such as H_2SO_4), it changes its elastic forces and swelling pressure, which in turn increases the membrane water uptake [58]. If the membrane is produced with basic ionomer material, it may also activate residual fluorinated side chain extremities

(SO_3F to SO_3H), to build the proton conductive end group [11]. This pre-treatment method is however rather cumbersome/time-consuming due to membrane swelling, handling issues, dimensional variability and therefore not well-suited for mass production [12].

3.1.3 Offline break-in: Membrane plasma sputter etching

Nguyen *et al*. tested the impact of different membrane pre-treatment methods on its surface ionic activity [59]. The ionic activity at the interface between the membrane and polymer phase in the CL has a significant impact on proton and water conductivity. Their tests included H_2O_2 wash (typically used to remove the membrane organic impurities [12], [54]), H_2SO_4 wash, as well as plasma sputter and reactive ion etching.

The first observation of Nguyen *et al*. was that the as-received Nafion membrane had lower surface activity than that calculated from its chemical formula. H_2O_2 wash and reactive ion etching further reduced the surface ionic activity, whilst H_2SO_4 wash had no negative impact. Sputter etching had the opposite effect, by increasing the surface ionic activity, close to what is expected from its calculated chemical formula.

Indeed, the sputter etching method removes the hydrophobic Teflon-rich skin layer of extruded Nafion membrane [59]. It also increases the membrane roughness, improving its contact with the CL, resulting in a better performance [11] (

FIGURE 4(a)). This skin structure change results in a membrane surface that may become hydrophobic quicker and remain so for a longer time after it has been in contact with liquid water.

3.1.4 Offline break-in: GDL compression

As previously stated, break-in causes geometrical distortion of the stack, which can be mostly assimilated to GDL deformation [60]. To compensate the loss of compression and maintain optimal ohmic contact resistance, the stack clamping pressure can be adjusted [51]. This can however increase mass transfer resistance, by partly intruding the GDL into the flow-field channels, resulting in maldistribution of reactant gasses [50]. General Motors presented a GDL pre-treatment method that resolves this issue [60].

Their method consists of cyclically deforming the GDL using a press, until it converges to a certain thickness. The number of required cycles and applied pressure depend on the GDL material softness level, as soft material is more prone to adopting a compressive set. Consequently, the total GDL deformation and therefore interfacial contact resistance increase will be much less significant during break-in. Furthermore, if the stack clamping pressure is adjusted, less and more uniform GDL intrusion occurs (

FIGURE 4(b)).

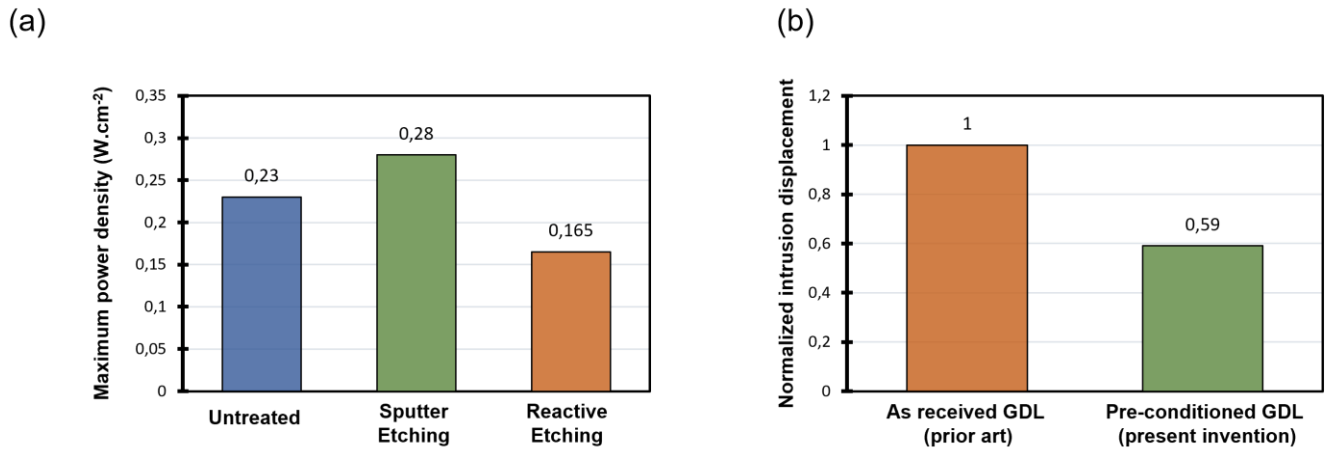

FIGURE 4. OFFLINE BREAK-IN METHODS: (A) EFFECT OF PLASMA ETCHING ON MEMBRANE SURFACE IONIC ACTIVITY AND FUEL CELL PERFORMANCE [59], (B) NORMALIZED INTRUSION DISPLACEMENT OF AS RECEIVED GDLS COMPARED TO PRECONDITIONED GDLS [60]

3.2 Break-in methods applied after final Fuel cell assembly (Online break-in)

This subsection regroups all “online” break-in methods, that are carried out right after the fuel cell stack is fully assembled. They are more or less polyvalent and unconventional. The methods used to accelerate the activation process are presented one by one, from the least to the most distant from the traditional methods.

3.2.1 Online break-in: Optimized load profile activation

During the online break-in procedure, current is typically drawn from the stack using an electronic load, which can be configured for galvanostatic or potentiostatic operation. When producing current/water, the proton conductive channel is generated within the ionomer [12], impurities are washed out and the polymer surface reorganizes. Traditional CC/CV (constant current/constant voltage) break-in profiles, such as presented by the U.S. Department Of Energy (DOE) or E.U. Joint Research Centre (JRC) typically consist of maintaining the mean cell voltage within a reduced range (0.45 to 0.75V) [61], [62]. This is to ensure fuel cell durability, as the priority of standardized activation protocols is to prevent cell degradation, regardless of its specifications.

Many novel CC/CV profiles have been proposed in the literature, in the hope to accelerate the break-in process [8], [63], [9], [64], [65]. The current or voltage range, and dynamic variations of those profiles vary. The "current stepping" profile presented by Yang *et al*. [63] is for example based on the current profile typically used for Polarization Curves (PolCurves). Using a dynamic CV profile, Yuan *et al*. managed to activate a stack in only 2 hours, by cycling from 0.3 to 0.6V, for 20 seconds per cycle [26]. By increasing the CV/CC profile range and/or frequency, the catalyst surface becomes subjected to oxidation/reduction processes, combined with the cycling of the generated water, desorbing and evacuating surface-blocking species [12]. Variable voltage/water production also accelerates the CL pore structure change, evacuation of unanchored particles and carbon black oxidation. Furthermore, as different potential levels trigger different specific activation mechanisms, having a dynamic load profile covering an important potential range is preferable [10].

The different impacts galvanostatic and potentiostatic activation have on break-in have also been studied in the literature [10], [9], [30]. All authors confirm that CV operation is preferable. At CV, the proton flow is more uniform over the membrane surface, even if the membrane water content is not homogenous. At CC, the protons only go through the already hydrated Nafion sections (

FIGURE 5(a)). Therefore, the activation mechanisms and water production rates are more uniform over the membrane surface with CV activation.

To conclude, the optimal load profile may be dynamic, cover an important voltage range, and be carried out in CV mode. This said, CC control is much simpler to implement on a test station, and increasing the cell voltage cycling range and frequency generates thermal, fluidic and electrical imbalances. The impact of these stressors on stack durability is discussed in further detail in the next section of this paper.

3.2.2 Online break-in: High temperature / pressure activation

According to PEM durability criteria, the cell and reactant temperatures must not exceed 75°C [66]. Almost all traditional break-in protocols (for cells using Nafion) respect these criteria, within a 5°C margin [9]. The cell pressure is also often limited to prevent mechanical failures or excessive reactant crossover.

The impact of the cell temperature and pressure conditions on activation time was first studied by Kaufman *et al*. on different types of MEAs [67], [68]. In each case, the elevated temperature and pressure resulted in shorter break-in times and better cell performance. Later studies confirmed the benefits ~~of~~ high cell temperatures have on activation time and performance, by testing cells up to 90°C [10] and 95°C [26]. More specifically, the decreasing trend of the membrane and polarization resistances with increasing temperatures have been elucidated through EIS measurements [26].

In the CL, the elevated pressure and temperature increases molecular agitation and therefore the pore opening rate and the ECSA. High temperatures also favour redox reactions (impurities/oxides desorption) and catalyst structure change kinetics (particle agglomeration, rounding...), resulting in an improved activity per site. This said, the maximum stack temperature should be limited (<100°C) to not affect the membrane crystallinity level (which could reduce ionomer water uptake [11]) and to avoid excessive water evaporation.

3.2.3 Online break-in: Supersaturated activation

Generating liquid water in the MEA during activation is essential to hydrate the polymer and change its structure, rearrange the surface skin, evacuate the Pt contaminants and non-bonded particles, etc. Therefore, the cell may be flooded in a “controlled” manner, to obtain liquid water without causing degradations.

Cho *et al*. propose the injection of water-saturated nitrogen for 2 hours to fully hydrate the ionomer [17]. An improved method, which guarantees liquid water formation within the stack, consists of injecting pure steam [57]. It can be categorized as the online variant of the MEA steaming method [56], without the CCM/sub-gasket deformation issues. As shown through EIS and Cyclic Voltammetry (CyV), cell steaming significantly reduces ohmic

and mass transfer resistances and increases the ECSA [57]. The low operation cost of this method is worth noting (no reactant consumption nor electric load), but it does require additional machinery (a vaporizer).

Temperature-controlled condensation methods have also been proposed in the literature, such as the "cooling after stop" technique [63]. This method simply consists of shutting down a stack and letting it passively cool down, without prior purging. An active rapid stack cooling variant of this method is presented in a Nissan patent [69]. The strategy applied in this patent slightly differs, as the stack is purged with dry reactants before cooling, and brought to an extremely low temperature (-1°C). With this strategy, water condensation is still significant during cooling, but there is no flooding risk upon restart. It however requires a temperature-controlled enclosure, or glycol cooling circuit, and presents risks of water freezing.

Temperature-controlled condensation techniques performed during stack operation also exist. Condensing during stack operation is hugely advantageous, as the current production-related mechanisms (presented in 3.2.1) occur simultaneously. Yang *et al*. propose to heat a stack to 60°C at the open circuit voltage (OCV), and then feed it with water-saturated reactants at 70°C while producing current, to force water condensation [63]. To avoid reactant depletion, the produced current must remain low. A variant of this method with more efficient heating is presented in a Toyota patent [70], where the calories are directly generated by the stack (called "heating power generation"). The phase where the water-saturated reactants are supplied is called "cleaning power generation" (

FIGURE 5(b)). During this phase, the variable cathode potential also desorbs impurities from the catalyst surface.

The Toyota patent variant of the supersaturated activation method is the best compromise between simplicity, efficiency, and versatility. This said, the “cooling after stop” technique may be suitable at the end of the break-in process, or when a shutdown phase is already foreseen during the protocol.

3.2.4 Online break-in: Short-circuit / pulsed activation

This method consists of accelerating the activation process by alternating between high power (e.g. short circuit) and low power (e.g. zero load) conditions. The high power phase is used to activate the stack, and the low

power phase is required for the stack to "recover". In short circuit, the stack is at full capacity (water and heat production, gas flowrate…). The ionomer and catalyst restructuring break-in morphological changes are therefore accelerated. The cyclic fluctuation of the cathode voltage is favourable for the reduction and oxidation of different surface-blocking species, and the high gas flowrate is ideal to evacuate them. Cyclic membrane swelling/shrinking may also be more efficient than constant high humidity conditions to accelerate the formation of a continuous water network [12].

To apply this method, Hyundai motor company [22] proposes to supply the fuel cell with reactants, connect it to a cooling circuit, and then connect a cable between the anode and cathode to generate a short circuit. The cell current is controlled by directly regulating the reactant supply (

FIGURE 5(c)). According to the authors, cell degradations are avoided by switching to a low power mode each time the cell voltage is reversed for more than 30 seconds. Based on this reasoning, a complete 30-minute protocol is proposed (with a low flowrate for 1 minute and then a high flowrate for 3 minutes, for 7 repetitions).

This said, nothing ensures that short circuiting for less than 30 seconds, and the reactant regulation power control method do not degrade the stack. The associated heat dissipation and the inhomogeneity within the stack, amplified by reactant depletion may severely impact durability (carbon corrosion, membrane thinning...). A less "extreme" variant of this method is proposed by Galitskaya *et al*. [23]. It aims to greatly accelerate break-in, whilst conserving stack durability. In this version, a load is used to alternate the fuel cell voltage between 0.1V (quasi-short circuit) and OCV. In their research, optimal durations for these two steps were determined (high power and OCV for 40 and 20 seconds, respectively).

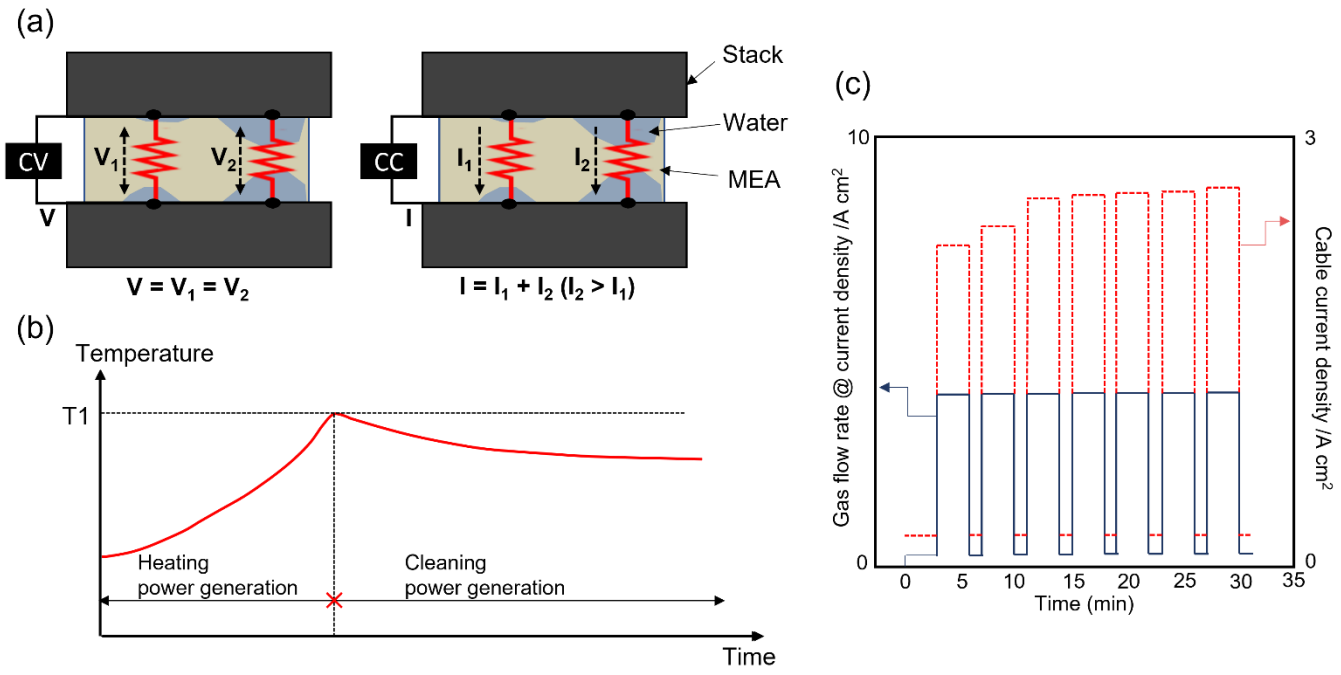

FIGURE 5. ONLINE BREAK-IN METHODS: (A) DIFFERENCE BETWEEN CV AND CC OPERATION PROTOCOLS [10], (B) SUPERSATURATED OPERATION PROTOCOL TEMPERATURE PROFILE [70], (C) SHORT-CIRCUIT PROTOCOL CURRENT PROFILE [22]

3.2.5 Online break-in: Air braking / starvation activation

The "Air braking / starvation" method consists of briefly drawing power from a fuel cell in the absence of oxidant. When oxygen is depleted, hydrogen partially reforms at the cathode (

FIGURE 6(a)), and the cell voltage progressively drops as the residual oxygen is consumed. Combined, low cell potential and hydrogen reforming create strong reducing conditions, therefore desorbing oxides and impurities from the catalyst surface. The absence of an air flow also increases the water molar fraction at the ionomer surface, as oxygen is consumed, and the produced water is not evacuated. Hydrogen reforming may also open pores leading to new active sites, or even enhance the TPB by irreversibly affecting the CL morphology (thickness) [19].

Ballard first applied this method, by simply supplying a fuel cell with reactants, requesting a current from a load, then cutting off the oxygen supply [71]. Balogun *et al.* propose a more compete version of this method, by also implementing high current and relaxation phases [20]. Additionally, a constant pressure gradient of 0.5 bar is imposed ($P_{anode} > P_{cathode}$), to force the passage of hydrogen to the cathode. The break-in mechanisms related to

high current and relaxation phases have been presented in the previous section (e.g ionomer restructuring, catalyst structure change, impurity desorption and evacuation). The reducing conditions at high current of the Balogun method (0.3V) are however not as strong as for the pulsed activation method (0 to 0.1V), in favour of cell durability. Starving the cathode of air and forcing hydrogen crossover however make up for this shortcoming, by generating even stronger reducing conditions.

Balongun *et al*. fully activated a 5cm^2 single cell in 40 minutes using their method (this said, more time may be necessary for large surface/number of cells stacks). Furthermore, if well controlled, contrary to the anode starvation method, cathode starvation can occur without degrading the cell [72]. Starving the cathode of air may also be applied on any test station, as it does not require additional machinery.

3.2.6 Online break-in: Reverse flow activation

Current production over the cell surface is typically not uniform, as a reactant concentration gradient exists between the gas inlet and outlet. This also induces a gradient in activation kinetics between the inlet and outlet regions, as observed by Park *et al*. on a segmented cell during activation . The reverse flow method aims to reach balanced activation over the cell surface, by periodically changing the flow direction of reactants. This can be achieved by “port reversal”, which consists of reversing the stack upside down (

FIGURE 6(b)), or “flow reversal” where the reactant inlet and outlet ports are permuted using quick connectors.

To determine the efficiency of the reverse flow activation, Park *et al*. activated two identical 5 cell stacks using a conventional break-in protocol (0.6V CV). Simultaneously, port reversal and then flow reversal was applied to one of the two stacks, resulting in a 43% activation time reduction, for similar final stack performance [66]. This said, reversing the stack upside down and/or permuting the reactants inlets/outlets is time consuming and might cause water management issues.

Another variant of this method named “air swing” uses a 4-way valve to periodically permute the cathode inlet and outlet during fuel cell operation (

FIGURE 6(c)) [74]. Reversing the flow direction using a 4-way valve is less time consuming, and eliminates the need of an air humidifier, by reinjecting the produced water in the cathode. Furthermore, as the cathode flow is

reversed during stack operation, it is temporarily starved of oxygen, triggering the cathode starvation-related break-in mechanisms presented in the previous section. The oxygen reduction and hydrogen reforming zones (see FIGURE 6(a)) also permute with the air swing method, resulting in a more uniform desorption of oxides and impurities.

Contrary to the Park *et al*. method, changing the anode flow direction by using a 4-way valve should not be promoted, due to the severe anode starvation-related degradations [75]. Even if only the cathode is starved stack durability is not ensured with the air swing method. Indeed, with the 4 way valve, the starvation process is never total and might cause voltage fluctuations, thus degrading the CL components [75]. The impact of these stressors on stack durability is discussed in further detail in the next section of this paper.

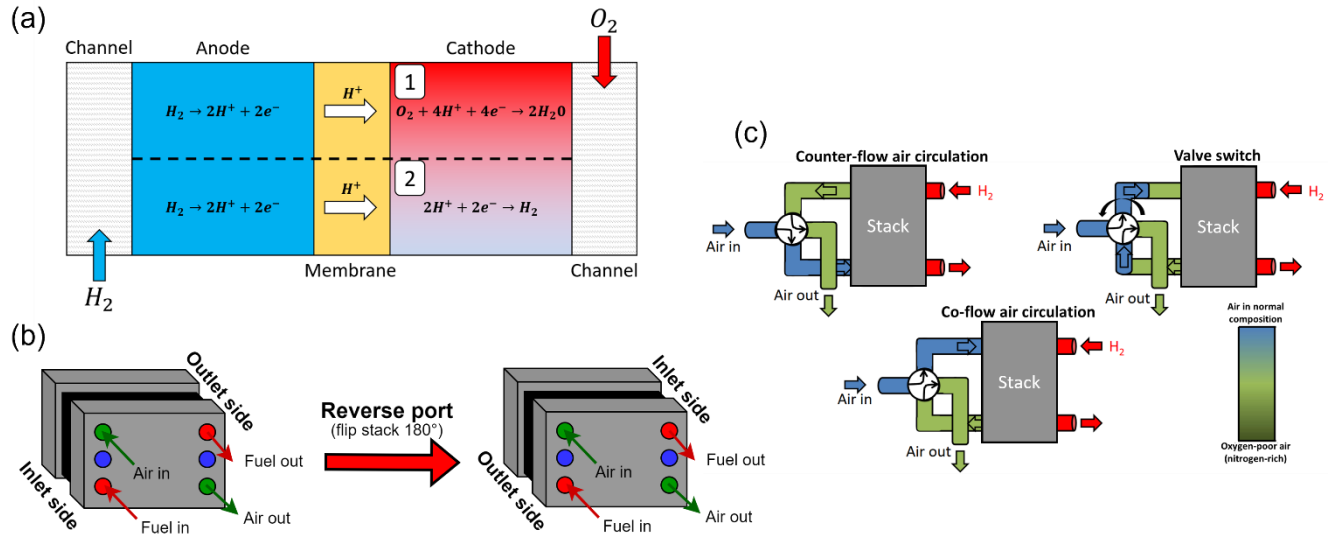

FIGURE 6. ONLINE BREAK-IN METHODS: (A) ILLUSTRATION OF TWO ZONES AT THE CELL CATHODE DURING AIR STARVATION, (B) PORT REVERSAL VARIANT OF THE REVERSE FLOW ACTIVATION METHOD [66], (C) AIR SWING PROTOCOL WORKING PRINCIPLE [74]

3.2.7 Online break-in: Hydrogen pumping activation

The hydrogen pumping method, traditionally used for hydrogen purification or high efficiency compression, can be used to increase fuel cell performance [13], [14]. This method consists of firstly purging the cathode with an inert gas and then closing the cathode inlet whilst keeping the outlet open. Afterwards, using an external power source, hydrogen is pumped. This consists of oxidizing hydrogen at the anode, transporting protons through the

membrane, and then reforming hydrogen at the cathode. This method has thus the potential to minimize hydrogen fuel loss, by recirculating it between the two compartments [12].

When pumping hydrogen, the hydrogen evolution reaction (HER) takes place at the cathode, whose activation mechanisms have been presented in the previous sections (

FIGURE 6(a)). Using an external power source to pump hydrogen however results in more uniform activation over the cell surface, as the HER zone expands over the entire cathode area (zone 2 of

Figure 6(a)). It however also implies that hydrogen pumping does not affect the ionomer structure, as no water is produced at the cathode (zone 1 of

Figure 6(a)).

He *et al*. proved that the release of hydrogen does not only reduce the catalyst surface-blocking species, but also significantly increases the CL porosity and tortuosity. For this, they pumped hydrogen for 20 minutes (by supplying 200mA.cm^{-2}), on a cell whose catalyst surface-blocking species had already been desorbed [15]. Additionally, CyV and PolCurve measurements were taken before and after hydrogen pumping. These measurements confirmed that hydrogen pumping significantly increased cell performance whilst not desorbing additional catalyst surface species, as the ECSA variation was negligible (Figure 7(a)). The ECSA measured through CyV only accounts for the contact surface between the catalyst and the electrolyte, not the accessibility of oxygen molecules. Therefore, the forced passage of hydrogen to the active sites must have created new pores, improving oxygen transport accessibility and thus cell performance.

3.2.8 Online break-in: Reactant switch activation

The reactant switch activation consists of generating oxidizing or reducing conditions within the cell without producing current, by adjusting the anode and/or cathode gas compositions. Ballard and Hyundai motor company for example propose to fill and expose the cathode to hydrogen or another reducing gas, followed by stack sealing and storage . The reducing atmosphere desorbs oxides and other impurities from the catalyst. Pre-heating and humidifying the gas may accelerate the desorption process, and hydrate the ionomer to a certain extend. Another strategy to expose the cathode to a reducing atmosphere consists of purging it of air and imposing a vacuum,

whilst supplying the anode with hydrogen [78]. The cathode fills with hydrogen, as the pressure difference forces H_2 crossover through the membrane (which may also affect CL porosity). With this setup, no direct hydrogen supply is required at the cathode input, but the pressure difference may tear the membrane.

TABLE 3. REACTANT SWITCH ACTIVATION STEPS [79]

	STEP	Gas On Anode	Gas On Cathode	Primary Load Swich	DC Power Supply Positive Terminal	Electrode Potential	Current Density	Time
Cathode Filling	1	100% H_2	N_2	Open	Not Connected	Cathode 0.95V to 0.00V	Zero	2 min.
Cycles	2	100% H_2	Air	Open	Not Connected	Cathode 0.00V to 0.95V	Zero	1.5 min.
	3	repeat step #1 followed by step #2 for total of 10 cycles						
Anode Filling	4	N_2	100% H_2	Open	Not Connected	Anode 0.95V to 0.00V	Zero	2 min.
Cycles	5	Air	100% H_2	Open	Not Connected	Anode 0.00V to 0.95V	Zero	1.5 min.
	6	repeat step #4 followed by step #5 for total of 10 cycles						
Performance Calibration	7	H_2	Air	Closed	Not Connected	Dependent on current density	0-1600 mASC	
	8	repeat step #7 up to 10 times						
Prior Art	1	H_2	Air	Closed	Not Connected	Dependent on current density	0-1000 mASC	
	2	repeat step #1 up to 10 times						

A more complete method presented by Schrooten *et al*. consists of cycling the electrodes potentials between 0 and 0.95V, through permutation between N_2, air and H_2 at the anode and cathode sides (**Erreur ! Source du renvoi introuvable.**) [79]. Complete oxidation and reduction cycles occur, to fully desorb the electrodes catalyst surface-blocking species. Exposing the cell to different gasses is a very cost-effective way to desorb those species and does not require a load. Consequently however, the previously presented current production-related activation mechanisms (membrane water network generation, impurity migration, side chain reorientation...) do not occur. This method also presents risks, in the case of an incomplete purge prior to a reactant switch step. The simultaneous presence of air and H_2 within the same volume, can severely degrade the cell (along the same mechanisms as those caused by H_2/O_2 crossover). Finally, the oxide/impurity desorption rates with these methods have slow kinetics. Therefore, methods such as hydrogen exposure may only be of interest to apply on assembled fuel cells during their storage period before they are put on an activation bench.

3.2.9 Online break-in: Cyclic Voltammetry activation

As previously stated, the amount and type of oxides/impurities coverage on the Pt surface is mixed [45] (PtOH, PtO, PtO_2, sub-surface oxides, airborne species [44], manufacturing residues [45], [47], etc.). Adsorption/desorption mechanisms strongly depend on the potential of the medium, and the ideal potential varies for each specie, depending on its nature and the desired reaction (oxidation/reduction). To efficiently reach each desorption potential, the CyV electrochemical characterization method may be used. Multiple oxides and impurities can be desorbed or transformed into less harmful molecular species with each potential sweep [71]. As the cell voltage is imposed by an external source, low cathode potentials can be reached without forcing short circuits or reactant starvations, and the maximum potential is not limited to OCV. In addition to catalyst impurity desorption, the consecutive oxidation/reduction cycles may also accelerate Pt particle rounding and agglomeration, increasing the ORR mass activity [49]. During the backwards potential sweep, the HER reaction occurs, which (as seen in the previous sections) affects the cathode CL porosity.

He *et al*. applied the hydrogen adsorption/desorption CyV method on pre-humidified cells (using water saturated N_2) [16], [17]. Only 23.2 minutes (30 cycles at $50mV.s^{-1}$ steps for a voltage range from 0.04 to 1.2V) were required to fully desorb the catalyst surface impurities. The CyV method efficiency may even further be improved by optimizing the potential scan rate, scan direction and amplitude. According to Shinozaki *et al*., increasing the scan rate (here $500mV.s^{-1}$) is favourable, as the number of cycles is a stronger accelerant for activation rather than the total duration [45]. Cycling up to 1.2V is also preferable, as at 1V (near OCV) some contaminants are not oxidized/removed, and at 1.4V the desorption rate is not improved and the cell degradation rate increases (Figure 7(b)).

Another CyV characterization method, named CO stripping, can also be applied to activate a fuel cell. It consists of firstly poisoning the cathode catalyst using a diluted nitrogen/CO mixture, and then cleaning it by oxidizing the absorbed CO [80]. By applying this method on an activated cell, Xu *et al*. managed to further increase its performance, by 29% [18], [15]. During CO contamination, a potentiostat imposes the cathode potential at 0.5V to favour CO absorption whilst preventing the HER (which would interfere with the results). After 30 minutes of cathode contamination, it is purged with pure nitrogen, and the adsorbed CO on the Pt is oxidized by CyV (between 0.5 and 1V to impede the HER). The first 3 potential cycles showed current peaks around 0.76V corresponding to the oxidation of CO into CO_2 (Figure 7(c)). During the 4th cycle, the absence of current peaks

confirmed total CO desorption. In addition to the cathode potential sweep, it is thought that when the CO oxidizes, it directly carries away a certain number of other species, accelerating the catalyst impurity desorption process [81].

There are durability concerns related to potential sweeping, as it can generate metallic cations, which in turn can decrease ionomer proton conductivity, and change electroosmotic drag. In-situ mitigation against contamination typically consists of increasing the cell water production rate [11]. However, drawing current is not possible during CyV. Consequently, the current production-related activation mechanisms do not occur. Similarly, potential levels up to and beyond OCV may also degrade the stack [82].

3.2.10 Online break-in: Compression cycles activation

The compression cycles activation is the only online method related to the mechanical break-in mechanisms. As previously stated, after assembly, the different cell elements have not had a chance to adapt and fit to each other's forms. Furthermore, during activation, irreversible microstructural deformations and variable water and heat production take place, altering the cell contact interface resistances.

Netwall *et al*. propose a mechanical break-in method, to apply after electrochemical activation [50]. It consist of firstly letting the cell undergo a compression and relaxation cycle using a mechanical press. This decreases the area-specific resistance, as the GDL is being formed into compression with the BP. Figure 7(d) is an example of three compressive load cycles, applied up to 1.4MPa. The first compression cycle exhibits the area resistance hysteresis as a function of compression stress, indicative of a mechanical break-in response. Subsequent compression/decompression cycles all follow the same path.

After the compression/decompression cycle, the cell is once again compressed and maintained at a fixed optimal compressive load. The optimal compressive stress must ensure low area-specific resistance and maintain of compression during fuel cell operation whilst preventing mechanical degradation of cell components. As seen on Figure 7(d), the area-specific resistance greatly decreases until 1MPa, and then slowly converges to a minimum value. Netwall *et al.* determined that a compressive stress of at least 1MPa is required to remove the temperature dependency on the area specific-resistance (for a fixed stress level below 1MPa, this resistance varies with

temperature). This said, stresses greater than 1.38MPa showed significant material damage, and negligible improvement in resistance. Therefore, the ideal compressive stress post break-in in their example is within the 1 to 1.38MPa range.

Some additional considerations should be taken when determining the optimal clamping pressure. Increasing compression inhibits mass transfer by reducing the GDL porosity [51], and by partly pushing the GDL material in the reactant flow channels [60]. Furthermore, compression also affects the membrane crystallization and ionic domain spacing, influencing water uptake [11]. This topic must be further studied.

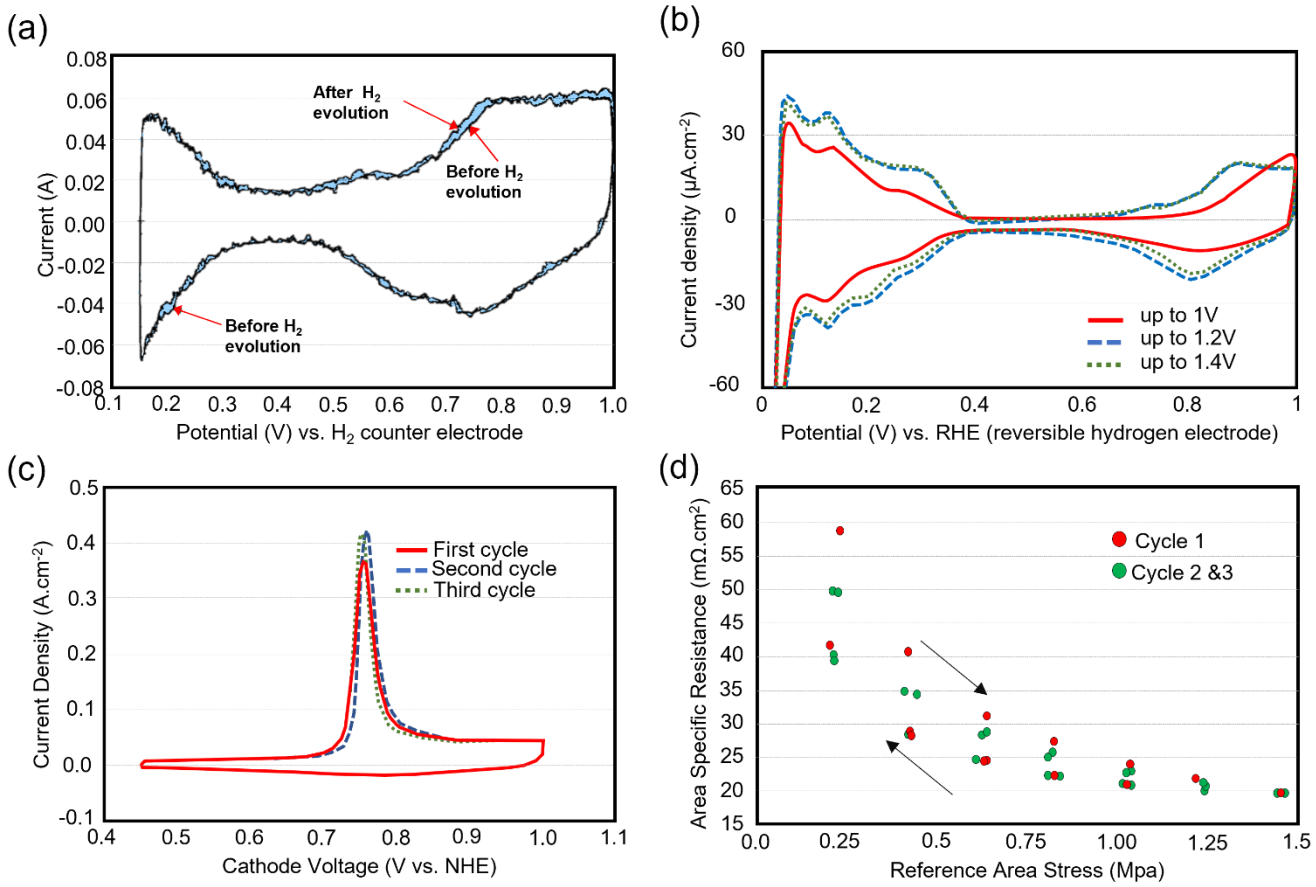

FIGURE 7. ONLINE BREAK-IN METHODS: (A) CYV CYCLES BEFORE AND AFTER HYDROGEN PUMPING [13], (B) EFFECTS OF MAXIMUM POTENTIAL DURING CYV BREAK-IN ON VOLTAMMOGRAM [45], (C) CV CYCLES USED TO OXIDIZE THE CO [18], (D) MECHANICAL BREAK-IN COMPRESSION CYCLES [50]

4 PEMFC break-in characterization

Break-in characterization, also named break-in monitoring or diagnosis consists of quantifying fuel cell activation evolution, completion, and cell component state of health.

There are two purposes related to fuel cell break-in characterization:

- **Standardization:** Obtaining accurately repeatable break-in protocols, by ensuring that no unexpected event has occurred during activation and guaranteeing iso-performance and durability. In addition to the post activation factory acceptance tests, it certifies that all delivered fuel cells to the customer meet specification requirements. It also guarantees that stacks dedicating to testing are fully conditioned, preventing inaccurate baseline metrics and misidentification of phenomena [13].
- **Benchmarking:** Comparing novel break-in protocols with the existing ones with respect to performance and impact on durability.

In this section, the traditional and novel PEMFC activation characterization methods are first presented. Afterwards, the limits related to break-in protocol benchmarking are discussed.

4.1 PEMFC break-in characterization methods

4.1.1 Break-in characterization: Traditional methods and limits

Traditionally, the metric used to quantify break-in evolution and completion is the cell voltage, tracked at a certain iso-current value, or vice versa. Several break-in completion criteria exist in the literature.

The most common criterion in the literature is based on performance convergence. For example, the US Fuel Cell Council defines it by a cell voltage deviation below 5mV between two measurements at 800mA.cm-2 [8]. In other cases, the criterion is poorly defined as “no further observable increase in performance” [9]. There is a lack of standardization in the literature with this criterion, as different threshold voltage/current deviation ($\Delta U/\Delta I$), and convergence time (Δt) values are used. Variable metrics (current/voltage/power) are also used to quantify break-in evolution, at different values, and scales (cell/stack). In the industry, another end-of-break-in criterion is often used and defined as reaching a certain performance threshold value. Both criteria are of little scientific rigor, as reaching a cell performance threshold value or convergence does not guarantee that it has completed its

morphological transformations. This has for example been proven with the CO-stripping method, which further activated a cell which had already reached stable performance [18].

A third criterion consists of waiting until the first decay in performance is observable, meaning that the stack is fully activated, as fuel cell ageing has started [12]. This criterion may be viable for traditional activation protocols, which are carried out using “safe” and stable operating conditions. Novel accelerated break-in methods however go against the durability guidelines, by causing flooding, starvations, applying high temperatures/pressures, high amplitude current/voltage fluctuations, etc. [28]. Even though activation increases cell performance, it does not mean that it is impervious to degradations.

Simultaneous fuel cell break-in and ageing has been observed in the literature (

FIGURE 8(a)) and is typically called over-conditioning [12]. Therefore, not only break-in but also ageing morphological changes should be monitored during activation. This is essential, as cell durability is one of the other hurdles that limits fuel cell mass production. It is however not simple to decorrelate break-in from ageing by tracking cell performance evolution, as the performance increase caused by fuel cell break-in hides the performance decrease caused by ageing. When testing novel break-in protocols, they can and should systematically be followed by an ageing protocol at least once. This is essential to precisely identify the long-term effects of the irreversible MEA microstructural changes caused by fuel cell break-in [83]. Post activation ageing protocols have been applied several times in the literature [20], [30] but not systematically, as they are costly and time consuming.

Using advanced (mostly electrochemical) characterization methods, break-in evolution, completion and impact on ageing can be quantified more precisely, and correlated with the activation and ageing mechanisms. These characterization methods, as well as the different morphological changes they can monitor are presented separately throughout the following subsections.

4.1.2 Break-in characterization: Polarization curve (PolCurve)

Polarization curves represent the fuel cell performance cartography over its entire operating range, by displaying the average steady-state cell voltage as a function of current density. The S-shaped PolCurve can be divided in three different regions, to evaluate the reaction rate, ohmic and mass transport losses evolution.

Reaction rate losses represent the energy required for the electrochemical reactions to take place on the catalyst surface and are therefore related to the ECSA and activity per site. By monitoring these losses, catalyst impurity desorption and structural changes (which affect the ORR reactions) can be quantified. The catalyst activity evolution can be further analysed by extracting specific parameters from the reaction rate losses expression [29]. Changes in Tafel slope are for example related to changes in Pt oxide coverage [41].

The ohmic resistance corresponds to the cumulative resistances of all cell components, but also the contact resistance between each component. Its evolution during activation can be related to the cell interfacial contact (mechanical activation), and the ionomer (water sorption and impurity evacuation).

Mass transfer losses are related to reactant and ion mobility to and from the active sites, and the available catalyst area and activity [29]. These losses evolve with GDL/CL porosity, removal of unanchored particles, the production of a water film on the catalyst surface and hydration of the ionomer surrounding the Pt.

4.1.3 Break-in characterization: Electrochemical Impedance spectroscopy (EIS)

The EIS is a powerful in-situ diagnostic method, typically carried out at 0.5, 1 or 1.5A.cm-2. It consists of adding a sinusoidal current perturbation to the base signal, which is swept over a large frequency range. On a Nyquist plot, the fuel cell losses can be dissociated from the frequential impedance response using an equivalent resistance/capacity model. Like PolCurves, it displays the ohmic (high frequency), kinetic (mid-frequency), and mass transfer (low frequency) losses in the fuel cell [73]. With the EIS method however, the different losses are better dissociated, and provide more precise measurements for one fixed current density. Additionally, the slope of the high frequency arc provides information regarding the CL and GDL pore shape and size [27]. Indeed, if the slope of high frequency arc of the Nyquist plot is steeper, the entrance of pores is larger.

The capacitance characteristics of an EIS curve are also indicators of the TPB area available for promoting catalytic reactions. They can be related to all morphological changes that increase the ECSA (such as PEM swelling, which generates a better connection between the three phases [83]).

4.1.4 Break-in characterization: Cyclic Voltammetry (CyV)

As previously stated, the CyV method can be used to activate and/or characterize a fuel cell. The area specific activity measured through CyV is an indicator of impurity levels that do not impede the accurate measurement of the ORR activity of Pt based catalysts [45]. Monitoring the evolution and stabilization of the kinetic, mixed and limiting current areas can therefore indicate the impurity desorption level (

FIGURE 8(b)).

Like EIS curves, voltammograms provide the value of the double layer capacitance [11]. Through the hydrogen adsorption and desorption areas, the ECSA value can also be specified, and the mean Pt particle size can be estimated [84]. With CyV, the permeation current (O_2 and H_2 crossover) can also be determined [85]. As reactant permeability through the membrane increases with water content [41] it is an image of its degree of activation. Additionally, H_2 crossover can be quantified using the linear sweep voltammetry (LSV) method, which consists of sweeping the voltage in a single direction, at a slower scan rate [29]. Combined with the Nernst equation and OCV measurements, the LSV method provides a precise estimation of the H_2 crossover rate.

4.1.5 Break-in characterization: Output gas / water composition analysis

Information regarding the stack degree of activation and state of health during break-in can be extracted from the cell anode/cathode output gas and water compositions.

Gas crossover rates and therefore membrane water content can be estimated by measuring the O_2 and H_2 flowrates at the anode and cathode outputs, respectively. Additionally, the concentration of different emissions (e.g. sulfate and other impurities) can be used to quantify ionomer and catalyst surface decontamination [73]. Similarly, fluor and hydrogen peroxide emissions can be related to ionomer and catalyst binder degradations [41],

[73], and CO_2 concentration to the degradation of the carbon support. With specific filters at the gas channel outputs, Pt particle loss related degradations may also be quantifiable.

4.1.6 Break-in characterization: Post-mortem

When carrying out a first full analysis of a novel break-in procedure, intrusive and destructive methods can be applied to observe cell materials evolution during activation and ageing.

The main component from which information can be drawn through microscope observations is the CL. More specifically catalyst characteristics such as Pt particle size, which evolve during break-in and ageing, can be quantified [30]. To determine the optimal clamping pressure for one stack configuration, post-mortem must also be used to quantify GDL material deformation / inclusion into the BP [50], [51].

4.2 PEMFC break-in protocols benchmarking and limits

As previously stated, fuel cell break-in characterization is essential for standardization, but also benchmarking purposes, to determine the optimal reproductible break-in protocol. When a novel break-in protocol is defined, it can be ranked to determine its performance relative to the other existing protocols.

4.2.1 Traditional PEMFC break-in protocols benchmarking and limits

To maximize break-in economic efficiency on a mass manufacturing scale, multiple metrics such as activation time, material and fuel cost, and impact on durability must be considered [10]. This said, industrial actors mostly focus on reducing break-in time and obtaining the best final cell performance (considered as the most important factors to reduce the fuel cell production cost per kW). Therefore, benchmarking as presented in the literature is often only based on those metrics [9], [11], [86] (

FIGURE 8(c)).

The process used in the literature to benchmark break-in methods is straightforward. Indeed, benchmarking tables are directly based on the experimental results provided by the different authors of the break-in methods in

their papers. However, these authors did not apply the same end-of-break-in criteria for their experiments. Therefore, it is not wise to draw conclusions based on these results. For improved benchmarking, the efficiency of each method must be revaluated experimentally, this time by using identical standardized advanced characterization methods as presented previously.

Apart from standardizing break-in characterization using advanced methods, there are several other "provisions" or "precautions" to be taken when comparing break-in methods. Indeed, the measured efficiency of a break-in protocol strongly depends on the characteristics of the used PEMFC. The main PEMFC characteristics which influence the benchmarking results are its materials, size, and manufacturing methods. These points are discussed one by one in the following subsection.

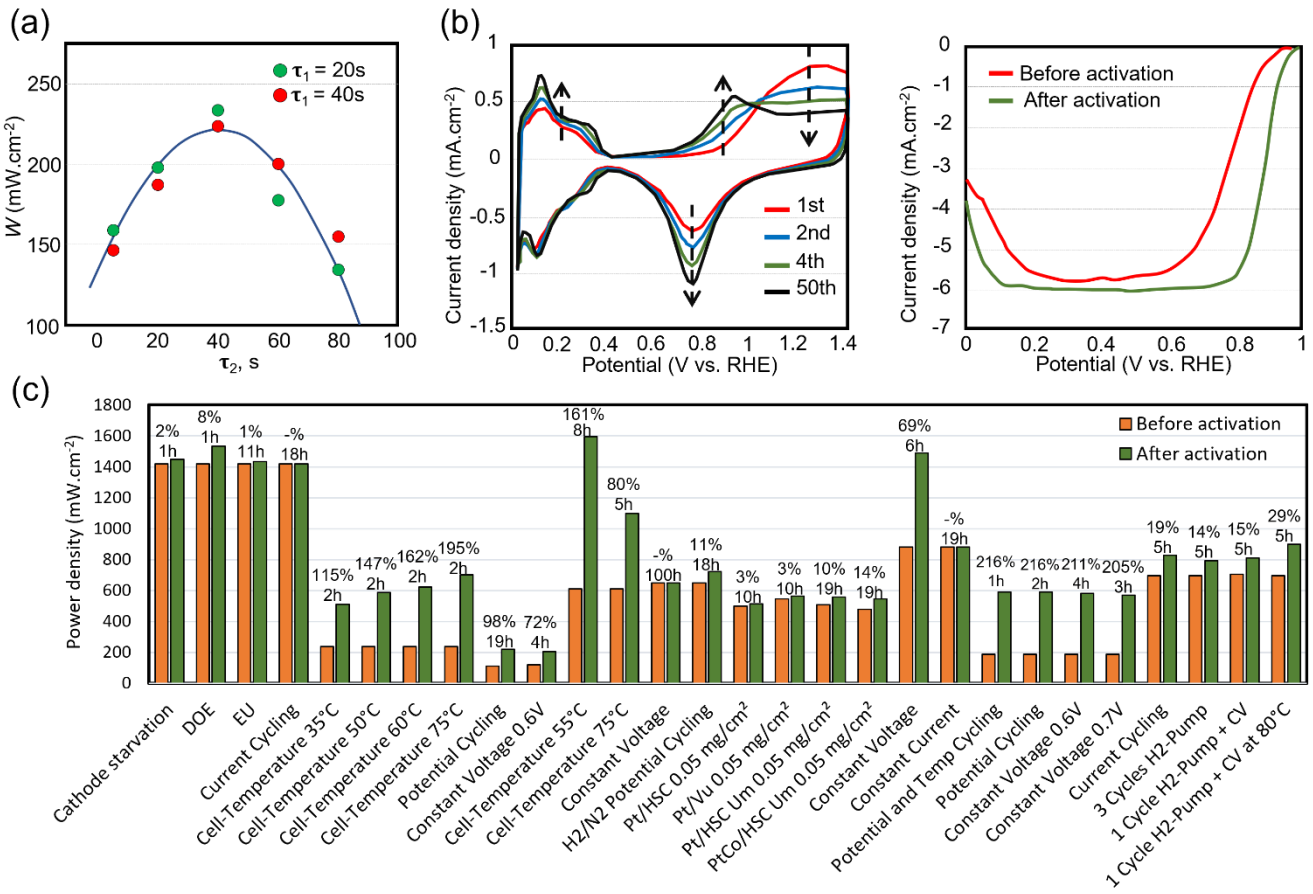

FIGURE 8. BREAK-IN CHARACTERIZATION AND BENCHMARKING: (A) EXAMPLE OF OVER-CONDITIONING WHEN INCREASING LOADING TIME (τ_2) ON PULSED ACTIVATION METHOD [23], (B) EXAMPLE OF IMPURITY DESORPTION DEGREE CHARACTERIZATION DURING BREAK-IN USING CYV [12] (C) EXAMPLE OF BREAK-IN METHODS BENCHMARKING (FROM VARIOUS SOURCES FROM LITERATURE) [11]

4.2.2 Impact of PEMFC characteristics on benchmarking results

The PEMFC stack dimensions (cell area / number of cells) greatly influence the efficiency of a break-in protocol [28]. On large stacks, reactant, water and heat distribution is less uniform over the cell surface, resulting in longer activation times. Furthermore, the efficiency order in which activation methods are ranked may also depend on the stack size. Indeed, break-in methods such as reverse activation (that focus on homogenizing activation over the cell surface) may be ranked higher if applied on large area cells. Similarly, the effect of compression cycles activation may be more noticeable on stacks with numerous cells.

The measured performance of a break-in method is also closely related to the PEMFC manufacturing method and used materials [31]. The time to condition a cell to its peak performance is unique for an electrode system and will depend to a great extent upon the CL. Variables and processes such as the used solvent ink formulation [87], drying and deposition technique, ionomer and carbon type and ionomer loading significantly impact the electrode morphology [12], [41]. This will in turn affects the evolution of proton conductivity, but also ECSA and mass transport losses during activation [11]. Impurity desorption disparities also exist between high loaded and low loaded electrodes, and the type of Pt-alloy [12], [41]. Therefore, different numbers of oxidation/reduction cycles are required to yield the peak performance.

Silva *et al*. observed variable break-in kinetics depending on membrane type and thickness [32]. More specifically, material characteristics like equivalent weight, side chain length, crystallinity, scavengers and reinforcements all affect the membrane morphological changes during activation [11]. The membrane water uptake characteristics in the free water regime (λ_F) during activation also depends on its manufacturing process (as it imprints a certain mechanical and thermal history). The proton conductivity increase rate also depends on the membrane additive dosage and formulation [37], [38]. Furthermore, if MEAs are directly bought from a manufacturer (not produced in-house) pre-treatment methods may already have been carried out by them. This information is typically not divulged. **Erreur ! Source du renvoi introuvable.** displays variable membrane pre-treatment method (boiling) efficiency, dependent on the type of membrane [32].

TABLE 4. MEMBRANE BOILING PRE-TREATMENT PERFORMANCE INCREASE, FOR DIFFERENT TYPES OF MEMBRANES [32]

Proton exchange membranes	**Proton conductivity/mS.cm^{-1}**		**Increase factor**
	Not pre-treated	Pre-treated	
Nafion 112	118.1	140.1	1.19
Nafion 1135	120.2	146.2	1.22
Nafion 117	132.9	159.2	1.20
sPEEK SD 42%	43.4	154.7	3.56
sPEEK ZrO_2 2.5 wt.%	33.5	88.9	2.65
sPEEK ZrO_2 5.0 wt.%	19.2	37.2	1.94

The BP surface roughness affects the resistive contact with the GDLs [50], and therefore the compression break-in cycle efficiency. The flow field layout (serpentine, parallel..) has also proven to influence break-in performance [88]. Finally, pre break-in cell storage conditions affect Pt [17] and ionomer [12] contamination and consequently activation time.

5 Conclusion

In this review paper, all different aspects of PEM fuel cell activation (e.g. break-in mechanisms, procedures, characterization, ageing...) have been covered, profoundly studied, and combined. The general findings of this work are the following:

(i) The morphological changes occurring within the PEMFC during activation have been disclosed. They are mostly related to the MEA electrochemistry. The membrane polymer hydrates, decontaminates and its inner structure and surface skin rearranges. In the CL, the pore structure opens, the polymer hydrates, carbon support oxidates, and the Pt structure reorganizes and decontaminates. These morphological changes directly affect cell properties such as porosity, catalyst size, shape and activity, polymer chain orientation and spacing, etc. The time constants associated with each mechanism range from a few seconds to multiple hours (or even days). Their cumulated contributions reduce the entire spectrum of fuel cell resistances (reaction rate, mass transfer and ohmic).

(ii) Numerous techniques exist to lower the activation time and cost. First, by pre-activating cell components (using steam, sulfuric acid, plasma, or compression), the time spent on an activation

bench can be reduced. The range of stressors of the stack break-in protocol may also simple be adjusted (dynamic load, potentiostatic, high temperature/pressure, supersaturated etc..), to improve its kinetics. Entirely new techniques to cycle between oxidizing and reducing conditions (short circuit, CyV, cathode starvation or reactant switch), uniformize activation over the cell surface (reverse flow, H2 pumping), or minimize resistance between cells (compression cycles) are the ones that have the most potential. Future optimized activation procedures will likely be based on a combination of cathode starvation, reverse flow and compression methods.

(iii) Developing the optimal reproductible activation protocol, based on the methods above is not a simple task. No standardized nor efficient processes are universally applied to characterize break-in evolution, completion, and impact on ageing. Better reproducibility can be achieved using advanced electrochemical characterization (PolCurve, EIS, CyV), combined with post-mortem and cell output species analysis. Using these same characterization methods, more precise benchmarking can also be achieved.

In addition to providing a fundamental basis for future "optimized" break-in research and development, the knowledge gaps related to fuel cell activation have also been elucidated throughout this paper. These shortcomings in the literature are summarized below, and are the main perspectives related to this work:

(i) Even though the main break-in physical principles have been identified, the claimed severity and duration of each mechanism remain debatable. Further detailed study of the break-in morphological changes in more specific disciplines (e.g. material science, fluid dynamics, mechanical science, electrochemistry...) is required. This research is also essential to understand how stack characteristics (e.g. assembly method, used materials...) affect break-in kinetics.

(ii) The impact of a break-in procedure on stack ageing is generally not sufficiently considered and must further be studied. This is especially true for "optimized" activation procedures as most stressors for accelerated break-in (e.g. cathode starvation, short-circuit…), are also stressors that induce degradations [28], [89]. Similarly, other break-in methods may extend the fuel cell durability beyond what is typically achieved with conventional activation procedures [20], [90], [91].

(iii) The advanced break-in characterization methods highlighted in this paper (PolCurve, EIS, CyV) remain non-ideal solutions. Indeed, these techniques are time consuming and directly interfere with the break-in measurements (as they simultaneously activate the stack). In other PEMFC-related research topics that have similar constraints (e.g. fault identification), non-intrusive diagnostic methods exist to overcome these barriers [92]–[94]. Such solutions (e.g. machine learning tools dedicated to fuel cell break-in diagnosis) are fully absent from the literature and should be developed.

Since break-in kinetics limitations (that do not degrade the stack) will undoubtedly be reached eventually, alternative options may be explored to further reduce the "need for break-in" on an activation bench. These include the optimization of various PEMFC manufacturing methods (e.g. catalyst ink composition, membrane additives dosing, cell components assembly and storage conditions adjustments…) [31]. Another ex-situ option which may soon be feasible is to finalize the activation of the fuel cell during its first hours of useful operation (e.g. while powering a fuel cell electric vehicle). Finally, as other fuel cell technologies, (e.g. Direct Methanol Fuel cells [14], Bio Fuels [95], [96]..) cell are also being actively developed, efforts towards their break-in or production acceptance tests must also be initiated.

6 Acknowledgments

This work has been supported by Symbio, a Faurecia Michelin hydrogen company.

This work has been supported by the EIPHI Graduate School (contract ANR-17-EURE-0002) and the Region Bourgogne Franche-Comté.

7 References

[1] S. T. Thompson *et al.*, "Direct hydrogen fuel cell electric vehicle cost analysis: System and high-volume manufacturing description, validation, and outlook," *J. Power Sources*, vol. 399, pp. 304–313, Sep. 2018, doi: 10.1016/j.jpowsour.2018.07.100.

[2] P. Costamagna and S. Srinivasan, "Quantum jumps in the PEMFC science and technology from the 1960s to the year 2000 Part I. Fundamental scientific aspects," *J. Power Sources*, p. 11, 2001.

[3] C. W. Wu, W. Zhang, X. Han, Y. X. Zhang, and G. J. Ma, "A systematic review for structure optimization and clamping load design of large proton exchange membrane fuel cell stack," *J. Power Sources*, vol. 476, p. 228724, Nov. 2020, doi: 10.1016/j.jpowsour.2020.228724.

[4] "Ballard wins extra funding to advance bus fuel cell modules," *Fuel Cells Bull.*, vol. 2013, no. 3, p. 9, Mar. 2013, doi: 10.1016/S1464-2859(13)70081-6.

[5] "DOE project funding for hybrid truck, fuel cell manufacturing QC," *Fuel Cells Bull.*, vol. 2015, no. 6, p. 11, Jun. 2015, doi: 10.1016/S1464-2859(15)30164-4.
[6] "Pragma secures extra funding to advance PEM fuel cells," *Fuel Cells Bull.*, vol. 2009, no. 10, p. 9, doi: 10.1016/S1464-2859(09)70330-X.
[7] T. Abergel, J. Armijo, and P. Bains, "Global Hydrogen review," *International Energy Agency*, p. 223, 2021.
[8] USFCC, "USFCC Single Cell Test Protocol # 05-014," Jul. 2006. [Online] Available: http://www.members.fchea.org/core/import/PDFs/Technical%20Resources/MatComp%20Single%20Cell%20Test%20Protocol%2005-014RevB.2%20071306.pdf
[9] M. Zhiani, S. Majidi, and M. M. Taghiabadi, "Comparative Study of On-Line Membrane Electrode Assembly Activation Procedures in Proton Exchange Membrane Fuel Cell," *Fuel Cells*, p. n/a-n/a, Aug. 2013, doi: 10.1002/fuce.201200139.
[10] M. S. Kim, J. H. Song, and D. K. Kim, "Development of Optimal Conditioning Method to Improve Economic Efficiency of Polymer Electrolyte Membrane (PEM) Fuel Cells," *Energies*, vol. 13, no. 11, p. 2831, Jun. 2020, doi: 10.3390/en13112831.
[11] K. Christmann, K. A. Friedrich, and N. Zamel, "Activation mechanisms in the catalyst coated membrane of PEM fuel cells," *Prog. Energy Combust. Sci.*, vol. 85, p. 100924, Jul. 2021, doi: 10.1016/j.pecs.2021.100924.
[12] S. S. Kocha and B. G. Pollet, "Advances in rapid and effective break-in/conditioning/recovery of automotive PEMFC stacks," *Curr. Opin. Electrochem.*, vol. 31, p. 100843, Feb. 2022, doi: 10.1016/j.coelec.2021.100843.
[13] C. He, Z. Qi, M. Hollett, and A. Kaufman, "An Electrochemical Method to Improve the Performance of Air Cathodes and Methanol Anodes," *Electrochem. Solid-State Lett.*, vol. 5, no. 8, p. A181, Jun. 2002, doi: 10.1149/1.1490715.
[14] Z. Qi and A. Kaufman, "Electrochemical Method to Improve the Performance of H2/Air PEM Fuel Cells and Direct Methanol Fuel Cells.," p. 7, 2004.
[15] Z. Xu, Z. Qi, C. He, and A. Kaufman, "Combined activation methods for proton-exchange membrane fuel cells," *J. Power Sources*, vol. 156, no. 2, pp. 315–320, May 2005, doi: https://doi.org/10.1016/j.jpowsour.2005.05.072.
[16] K. Y. Cho, "Method of activating membrane electrode assembly (PEM) of polymer electrolyte membrane fuel cell (PEMFC) using cyclic voltammetry (CV)," US 2009/0155635A1, Jun. 2009
[17] K.-Y. Cho and H.-Y. Jung, "Application of CV cycling to the activation of the polymer electrolyte membrane fuel cell," vol. 23, pp. 445–449, 2012.
[18] Z. Xu, Z. Qi, and A. Kaufman, "Activation of proton-exchange membrane fuel cells via CO oxidative stripping," *J. Power Sources*, vol. 156, no. 2, pp. 281–283, Feb. 2005, doi: https://doi.org/10.1016/j.jpowsour.2005.02.094.
[19] J. hee Song, M. soo Kim, Y. rim Kang, and D. kyu Kim, "Study on a drasitically hydrogen consumption saving conditioning method for Polymer electrolyte membrane fuel cell," *J. Energy Storage*, vol. 44, p. 103338, Dec. 2021, doi: 10.1016/j.est.2021.103338.
[20] E. Balogun, A. O. Barnett, and S. Holdcroft, "Cathode starvation as an accelerated conditioning procedure for perfluorosulfonic acid ionomer fuel cells," *J. Power Sources Adv.*, vol. 3, p. 100012, Jun. 2020, doi: 10.1016/j.powera.2020.100012.
[21] D. Yang, "Rapid activation of a full-length proton exchange membrane fuel cell stack with a novel intermittent oxygen starvation method," p. 9, 2022.
[22] S. Ik Jae *et al.*, "Apparatus and method for acceleratively activating fuel cell," Sep. 2011
[23] E. Galitskaya *et al.*, "Pulsed Activation of a Fuel Cell on the Basis of a Proton-Exchange Polymer Membrane," *Tech. Phys. Lett.*, vol. 44, pp. 570–573, Aug. 2018, doi: 10.1134/S1063785018070064.
[24] D. Wang, X. Ding, D. Yang, Z. Liang, and L. Wang, "A novel high current pulse activation method for proton exchange membrane fuel cell," *AIP Adv.*, vol. 11, no. 5, p. 055004, May 2021, doi: 10.1063/5.0046879.
[25] F. Van der Linden, E. Pahon, and S. Morando, "Rodage accéléré de pile à combustible de type PEM," in *Symposium de Génie Electrique*, Jul. 2021, p. 9. doi: hal-03359936.
[26] X.-Z. Yuan, J. C. Sun, H. Wang, and H. Li, "Accelerated conditioning for a proton exchange membrane fuel cell," *J. Power Sources*, vol. 205, pp. 340–344, Jan. 2012, doi: https://doi.org/10.1016/j.jpowsour.2012.01.039.
[27] J.-M. Jang, G.-G. Park, Y.-J. Sohn, S.-D. Yim, C.-S. Kim, and T.-H. Yang, "The Analysis on the Activation Procedure of Polymer Electrolyte Fuel Cells," *J. Electrochem. Sci. Technol.*, vol. 2, no. 3, pp. 131–135, Sep. 2011, doi: 10.33961/JECST.2011.2.3.131.
[28] P. Pei, X. Fu, Z. Zhu, P. Ren, and D. Chen, "Activation of polymer electrolyte membrane fuel cells: Mechanisms, procedures, and evaluation," *Int. J. Hydrog. Energy*, p. S0360319922023850, Jun. 2022, doi: 10.1016/j.ijhydene.2022.05.228.
[29] V. Silva, "Polymer electrolyte membrane fuel cells : activation analysis and operating conditions optimization," University of Porto FEUP, Porto, 2009.
[30] M. M. Taghiabadi, M. Zhiani, and V. Silva, "Effect of MEA activation method on the long-term performance of PEM fuel cell," *Appl. Energy*, vol. 242, pp. 602–611, Mar. 2019, doi: https://doi.org/10.1016/j.apenergy.2019.03.157.
[31] F. Van der Linden, E. Pahon, S. Morando, and D. Bouquain, "Optimizing Proton Exchange Membrane Fuel Cell manufacturing process to reduce break-in time," in *2020 IEEE Vehicle Power and Propulsion Conference (VPPC)*, Gijon, Spain: IEEE, Nov. 2020, pp. 1–5. doi: 10.1109/VPPC49601.2020.9330846.
[32] V. B. Silva and A. Rouboa, "An activation procedure applied to fluorinated and non-fluorinated proton exchange membranes," *Fuel Process. Technol.*, vol. 103, pp. 27–33, Mar. 2012, doi: https://doi.org/10.1016/j.fuproc.2011.12.042.

[33] R. P. O'Hayre, S.-W. Cha, W. G. Colella, and F. B. Prinz, *Fuel cell fundamentals*, Third edition. Hoboken, New Jersey: Wiley, 2016.
[34] A. Kusoglu and A. Z. Weber, "Water Transport and Sorption in Nafion Membrane," in *ACS Symposium Series*, K. A. Page, C. L. Soles, and J. Runt, Eds., Washington, DC: American Chemical Society, 2012, pp. 175–199. doi: 10.1021/bk-2012-1096.ch011.
[35] S. Ueda, S. Koizumi, and Y. Tsutsumi, "Initial conditioning of a polymer electrolyte fuel cells: The relationship between microstructure development and cell performance, investigated by small-angle neutron scattering," *Results Phys.*, vol. 12, pp. 1871–1879, Jan. 2019, doi: https://doi.org/10.1016/j.rinp.2019.01.066.
[36] F. Van Der Linden, E. Pahon, S. Morando, and D. Bouquain, "Proton-exchange membrane fuel cell ionomer hydration model using finite volume method," *Int. J. Hydrog. Energy*, p. S0360319922019838, May 2022, doi: 10.1016/j.ijhydene.2022.05.012.
[37] N. Zhao, Z. Xie, and Z. Shi, "Understanding of Nafion Membrane Additive Behaviors in Proton Exchange Membrane Fuel Cell Conditioning," *J. Electrochem. Energy Convers. Storage*, vol. 16, no. 1, p. 011011, Feb. 2019, doi: 10.1115/1.4040827.
[38] N. Zhao *et al.*, "Effects of Membrane Additives on PEMFC Conditioning," *ChemistrySelect*, vol. 4, no. 43, pp. 12649–12655, Nov. 2019, doi: 10.1002/slct.201903623.
[39] Z. Jingxin, "Methods and processes to recover voltage loss of pem fuel cell stack" US20110195324A1
[40] V. Yarlagadda *et al.*, "Boosting Fuel Cell Performance with Accessible Carbon Mesopores," *ACS Energy Lett.*, vol. 3, no. 3, pp. 618–621, Mar. 2018, doi: 10.1021/acsenergylett.8b00186.
[41] S. Kabir *et al.*, "Elucidating the Dynamic Nature of Fuel Cell Electrodes as a Function of Conditioning: An ex Situ Material Characterization and in Situ Electrochemical Diagnostic Study," *ACS Appl. Mater. Interfaces*, vol. 11, no. 48, pp. 45016–45030, Dec. 2019, doi: 10.1021/acsami.9b11365.
[42] A. Kongkanand and M. F. Mathias, "The Priority and Challenge of High-Power Performance of Low-Platinum Proton-Exchange Membrane Fuel Cells," *J. Phys. Chem. Lett.*, vol. 7, no. 7, pp. 1127–1137, Apr. 2016, doi: 10.1021/acs.jpclett.6b00216.
[43] I. Jiménez-Morales *et al.*, "Correlation between the surface characteristics of carbon supports and their electrochemical stability and performance in fuel cell cathodes," *Carbon Energy*, vol. 3, no. 4, pp. 654–665, Aug. 2021, doi: 10.1002/cey2.109.
[44] X. Cheng *et al.*, "A review of PEM hydrogen fuel cell contamination: Impacts, mechanisms, and mitigation," *J. Power Sources*, vol. 165, no. 2, pp. 739–756, Mar. 2007, doi: 10.1016/j.jpowsour.2006.12.012.
[45] K. Shinozaki, J. W. Zack, R. M. Richards, B. S. Pivovar, and S. S. Kocha, "Oxygen Reduction Reaction Measurements on Platinum Electrocatalysts Utilizing Rotating Disk Electrode Technique: I. Impact of Impurities, Measurement Protocols and Applied Corrections," *J. Electrochem. Soc.*, vol. 162, no. 10, pp. F1144–F1158, 2015, doi: 10.1149/2.1071509jes.
[46] J. Park and D. Kim, "Effect of cerium/18-crown-6-ether coordination complex OH quencher on the properties of sulfonated poly(ether ether ketone) fuel cell electrolyte membranes," *J. Membr. Sci.*, vol. 469, pp. 238–244, Nov. 2014, doi: 10.1016/j.memsci.2014.06.044.
[47] K. Palanichamy, A. Prasad, and S. Advani, "Off-Line Conditioning of PEM Fuel Cell Membrane," *ECS Meet. Abstr.*, Oct. 2008, [Online]. Available: http://ma.ecsdl.org/content/MA2008-02/11/1091.abstract
[48] J. M. Moore, P. L. Adcock, J. B. Lakeman, and G. O. Mepsted, "The effects of battlefield contaminants on PEMFC performance," p. 7, 2000.
[49] D. E. Ramaker, A. Korovina, V. Croze, J. Melke, and C. Roth, "Following ORR intermediates adsorbed on a Pt cathode catalyst during break-in of a PEM fuel cell by in operando X-ray absorption spectroscopy," *Phys Chem Chem Phys*, vol. 16, no. 27, pp. 13645–13653, 2014, doi: 10.1039/C4CP00192C.
[50] C. J. Netwall, B. D. Gould, J. A. Rodgers, N. J. Nasello, and K. E. Swider-Lyons, "Decreasing contact resistance in proton-exchange membrane fuel cells with metal bipolar plates," *J. Power Sources*, vol. 227, pp. 137–144, Apr. 2013, doi: 10.1016/j.jpowsour.2012.11.012.
[51] W. R. Chang, J. J. Hwang, F. B. Weng, and S. H. Chan, "Effect of clamping pressure on the performance of a PEM fuel cell," *J. Power Sources*, vol. 166, no. 1, pp. 149–154, Mar. 2007, doi: 10.1016/j.jpowsour.2007.01.015.
[52] A. Therdthianwong, P. Manomayidthikarn, and S. Therdthianwong, "Investigation of membrane electrode assembly (MEA) hot-pressing parameters for proton exchange membrane fuel cell," *Energy*, vol. 32, no. 12, pp. 2401–2411, Dec. 2007, doi: 10.1016/j.energy.2007.07.005.
[53] V. Mehta and J. S. Cooper, "Review and analysis of PEM fuel cell design and manufacturing," *J. Power Sources*, p. 22, 2003.
[54] Z. Qi and A. Kaufman, "Enhancement of PEM fuel cell performance by steaming or boiling the electrode," *J. Power Sources*, vol. 109, no. 1, pp. 227–229, Jan. 2002, doi: https://doi.org/10.1016/S0378-7753(02)00060-5.
[55] G. Alberti, R. Narducci, and M. Sganappa, "Effects of hydrothermal/thermal treatments on the water-uptake of Nafion membranes and relations with changes of conformation, counter-elastic force and tensile modulus of the matrix," *J. Power Sources*, vol. 178, no. 2, pp. 575–583, Apr. 2008, doi: 10.1016/j.jpowsour.2007.09.034.
[56] S. Paul, "3M Innovative Properties Company Patent US7608118B2 – 2009 - Preconditioning Fuel cell membrane electrode asseblies," p. 8.

[57] M. Zhiani, I. Mohammadi, and S. Majidi, “Membrane electrode assembly steaming as a novel pre-conditioning procedure in proton exchange membrane fuel cell,” *Int. J. Hydrog. Energy*, vol. 42, no. 7, pp. 4490–4500, Feb. 2017, doi: 10.1016/j.ijhydene.2017.01.103.
[58] J. Parrondo, M. Ortueta, and F. Mijangos, “SWELLING BEHAVIOUR OF PEMFC DURING CONDITIONING,” *Braz. J. Chem. Eng.*, vol. 24, no. 03, p. 9, 2007.
[59] T. Van Nguyen, M. Vu Nguyen, K. J. Nordheden, and W. He, “Effect of Bulk and Surface Treatments on the Surface Ionic Activity of Nafion Membranes,” *J. Electrochem. Soc.*, vol. 154, no. 11, p. A1073, 2007, doi: 10.1149/1.2781247.
[60] R. Pinkhas, “US8415076 Preconditioning of gas diffusion layers for improved performance and operational stability of PEM fuel cells,” Nov. 2015
[61] G. Tsotridis, A. Pilenga, G. De Marco, T. Malkow, European Commission, and Joint Research Centre, *EU harmonised test protocols for PEMFC MEA testing in single cell configuration for automotive applications.* Luxembourg: Publications Office, 2015. Accessed: Nov. 12, 2019. [Online]. Available: http://bookshop.europa.eu/uri?target=EUB:NOTICE:LDNA27632:EN:HTML
[62] “U.S. Department of Energy, DoE Procedures for Performing PEM Single Cell Testing, 2009, p. 47. # DE-FC36-06GO16028 April 8.”
[63] C. Yang, M. Hu, C. Wang, and G. Cao, “A three-step activation method for proton exchange membrane fuel cells,” *J. Power Sources*, vol. 197, pp. 180–185, Sep. 2011, doi: https://doi.org/10.1016/j.jpowsour.2011.09.038.
[64] R. Cuccaro, M. Lucariello, A. Battaglia, and A. Graizzaro, “Research of a HySyLab internal standard procedure for single PEMFC,” *Int. J. Hydrog. Energy*, vol. 33, no. 12, pp. 3159–3166, Apr. 2008, doi: https://doi.org/10.1016/j.ijhydene.2008.04.016.
[65] T. Malkow, G. De Marco, A. Pilenga, M. Honselaar, and G. Tsotridis, “Testing the voltage and power as function of current density. Test Module PEFC SC 5-2,” JRC (Joint Research Centre, Institute for Energy), Petten, Apr. 2010. [Online]. Available: https://ec.europa.eu/jrc/sites/jrcsh/files/polarisation_curve_testprocedure.pdf
[66] F. A. de Bruijn, V. A. T. Dam, and G. J. M. Janssen, “Review: Durability and Degradation Issues of PEM Fuel Cell Components,” *Fuel Cells*, vol. 8, no. 1, pp. 3–22, Feb. 2008, doi: 10.1002/fuce.200700053.
[67] Z. Qi and A. Kaufman, “Quick and effective activation of proton-exchange membrane fuel cells,” *J. Power Sources*, vol. 114, no. 1, pp. 21–31, Oct. 2003, doi: https://doi.org/10.1016/S0378-7753(02)00587-6.
[68] Z. Qi and A. Kaufman, “Activation of low temperature PEM fuel cells,” *J. Power Sources*, vol. 111, no. 1, pp. 181–184, May 2002, doi: https://doi.org/10.1016/S0378-7753(02)00273-2.
[69] N. Matsuoka and R. Shimoi, “Fuel cell conditioning system and related method,” 2005
[70] K. Kodama, “Method of running in operation of a fuel cell,” 2017
[71] R. H. Barton and U. S. Cl, “Conditioning and maintenance methods for fuel cells,” US 2003/0224227A1, 2003
[72] M. Gerard, J.-P. Poirot-Crouvezier, D. Hissel, and M.-C. Pera, “Oxygen starvation analysis during air feeding faults in PEMFC,” *Int. J. Hydrog. Energy*, vol. 35, no. 22, pp. 12295–12307, Nov. 2010, doi: 10.1016/j.ijhydene.2010.08.028.
[73] J. Y. Park, I. S. Lim, E. J. Choi, Y. H. Lee, and M. S. Kim, “Comparative study of reverse flow activation and conventional activation with polymer electrolyte membrane fuel cell,” *Renew. Energy*, vol. 167, pp. 162–171, Apr. 2021, doi: 10.1016/j.renene.2020.11.069.
[74] B. Decoopman, “Compréhension des mécanismes de dégradation des cœurs de pile à combustible PEM en application automobile.” hal id: tel-02990129
[75] M. Gerard, J.-P. Poirot-Crouvezier, D. Hissel, and M.-C. Pe´ra, “Oxygen Starvation Effects on PEMFC Durability,” in *FUELCELL2010*, ASME 2010 8th International Fuel Cell Science, Engineering and Technology Conference: Volume 1, juin 2010, pp. 593–600. doi: 10.1115/FuelCell2010-33173.
[76] J. H. L. Hyun Suk Choo, “Pre-activation method for fuel cell stack.pdf,” Feb. 2014
[77] B. G. NengYou Jia, “Conditioning method for fuel cells,” May 2002
[78] H. S. Choo, “Method for activating Fuel cell stack without using electronic load,” US20160164132A1
[79] J. A. Schrooten, J. M. Marzullo, and M. L. Perry, “Performance enhancing Break-in method for a PEM fuel cell,” US 7,078,118B2
[80] H. Wang, “PEM Fuel Cell Diagnostic Tools,” p. 556.
[81] K. Masahito, “Ageing method of Fuel cell,” US 2020/0099071 A1
[82] S. Sugawara *et al.*, “Performance decay of proton-exchange membrane fuel cells under open circuit conditions induced by membrane decomposition,” *J. Power Sources*, vol. 187, no. 2, pp. 324–331, Feb. 2009, doi: 10.1016/j.jpowsour.2008.11.021.
[83] M. Zhiani and S. Majidi, “Effect of MEA conditioning on PEMFC performance and EIS response under steady state condition,” *Int. J. Hydrog. Energy*, vol. 38, no. 23, pp. 9819–9825, Aug. 2013, doi: 10.1016/j.ijhydene.2013.05.072.
[84] V. B. Silva and A. Rouboa, “Hydrogen-fed PEMFC: Overvoltage analysis during an activation procedure,” *J. Electroanal. Chem.*, vol. 671, pp. 58–66, Feb. 2012, doi: https://doi.org/10.1016/j.jelechem.2012.02.013.
[85] S. Wasterlain, “Approches experimentales et analyse probabiliste pour le diagnostic de piles a combustible de type PEM,” 2010 hal id: tel-00474356.
[86] X.-Z. Yuan, S. Zhang, J. C. Sun, and H. Wang, “A review of accelerated conditioning for a polymer electrolyte membrane fuel cell,” *J. Power Sources*, vol. 196, no. 22, pp. 9097–9106, Jun. 2011, doi: https://doi.org/10.1016/j.jpowsour.2011.06.098.

[87] S.-J. Shin, J.-K. Lee, H.-Y. Ha, S.-A. Hong, H.-S. Chun, and I.-H. Oh, "Effect of the catalytic ink preparation method on the performance of polymer electrolyte membrane fuel cells," *J. Power Sources*, vol. 106, no. 1–2, pp. 146–152, Apr. 2002, doi: 10.1016/S0378-7753(01)01045-X.
[88] I. Alaefour, S. Shahgaldi, A. Ozden, X. Li, and F. Hamdullahpur, "The role of flow-field layout on the conditioning of a proton exchange membrane fuel cell," *Fuel*, vol. 230, pp. 98–103, Oct. 2018, doi: 10.1016/j.fuel.2018.05.062.
[89] J. Wu *et al.*, "A review of PEM fuel cell durability: Degradation mechanisms and mitigation strategies," *J. Power Sources*, vol. 184, no. 1, pp. 104–119, Sep. 2008, doi: 10.1016/j.jpowsour.2008.06.006.
[90] Y. Zhan, Y. Guo, J. Zhu, and L. Li, "Current short circuit implementation for performance improvement and lifetime extension of proton exchange membrane fuel cell," *J. Power Sources*, vol. 270, pp. 183–192, Dec. 2014, doi: 10.1016/j.jpowsour.2014.07.104.
[91] J. Mitzel, Q. Zhang, P. Gazdzicki, and K. A. Friedrich, "Review on mechanisms and recovery procedures for reversible performance losses in polymer electrolyte membrane fuel cells," *J. Power Sources*, vol. 488, p. 229375, Mar. 2021, doi: 10.1016/j.jpowsour.2020.229375.
[92] H. Wang, S. Morando, A. Gaillard, and D. Hissel, "Sensor development and optimization for a proton exchange membrane fuel cell system in automotive applications," *J. Power Sources*, vol. 487, p. 229415, Mar. 2021, doi: 10.1016/j.jpowsour.2020.229415.
[93] E. Dijoux, N. Y. Steiner, M. Benne, M.-C. Péra, and B. G. Pérez, "A review of fault tolerant control strategies applied to proton exchange membrane fuel cell systems," *J. Power Sources*, vol. 359, pp. 119–133, Aug. 2017, doi: 10.1016/j.jpowsour.2017.05.058.
[94] L. A. M. Riascos, M. G. Simoes, and P. E. Miyagi, "On-line fault diagnostic system for proton exchange membrane fuel cells," *J. Power Sources*, vol. 175, no. 1, pp. 419–429, Jan. 2008, doi: 10.1016/j.jpowsour.2007.09.010.
[95] E. Andriukonis, R. Celiesiute-Germaniene, S. Ramanavicius, R. Viter, and A. Ramanavicius, "From Microorganism-Based Amperometric Biosensors towards Microbial Fuel Cells," *Sensors*, vol. 21, no. 7, p. 2442, Apr. 2021, doi: 10.3390/s21072442.
[96] S. Ramanavicius and A. Ramanavicius, "Conducting Polymers in the Design of Biosensors and Biofuel Cells," *Polymers*, vol. 13, no. 1, p. 49, Dec. 2020, doi: 10.3390/polym13010049.